



This is a repository copy of *Mechanisms and Mitigation of Agglomeration during Fluidized Bed Combustion of Biomass: A Review*.

White Rose Research Online URL for this paper:
<http://eprints.whiterose.ac.uk/131275/>

Version: Accepted Version

Article:

Morris, J., Daood, S. orcid.org/0000-0002-4580-2504, Chilton, S. et al. (1 more author) (2018) Mechanisms and Mitigation of Agglomeration during Fluidized Bed Combustion of Biomass: A Review. *Fuel*, 230. pp. 452-473. ISSN 0016-2361

<https://doi.org/10.1016/j.fuel.2018.04.098>

Reuse

This article is distributed under the terms of the Creative Commons Attribution-NonCommercial-NoDerivs (CC BY-NC-ND) licence. This licence only allows you to download this work and share it with others as long as you credit the authors, but you can't change the article in any way or use it commercially. More information and the full terms of the licence here: <https://creativecommons.org/licenses/>

Takedown

If you consider content in White Rose Research Online to be in breach of UK law, please notify us by emailing eprints@whiterose.ac.uk including the URL of the record and the reason for the withdrawal request.



eprints@whiterose.ac.uk
<https://eprints.whiterose.ac.uk/>

1 Mechanisms and Mitigation of Agglomeration during Fluidized Bed

2 Combustion of Biomass: A Review

3 Jonathan D. Morris^a, Syed Sheraz Daood^{a*}, Stephen Chilton^b, William Nimmo^a

4 ^a*Energy Engineering Group, Energy 2050, Department of Mechanical Engineering, University of*
5 *Sheffield, Sheffield S10 2TN, UK*

6 ^b*Sembcorp Utilities UK Ltd., Sembcorp U.K. Headquarters, Wilton International, Middlesbrough TS90*
7 *8WS, United Kingdom*

8 **Corresponding author at: Level 1, Arts Tower, Energy Engineering Group, Energy 2050, Department*
9 *of Mechanical Engineering, University of Sheffield, Sheffield S10 2TN, UK.*

10 *E-mail address: s.daood@sheffield.ac.uk (S.S. Daood)*

11 Abstract

12 A key issue associated with Fluidized Bed Combustion of biomass is agglomeration. The presence of
13 high quantities of alkali species in biomass ash leads to the formation of sticky alkali-silicate liquid
14 phases during combustion, and consequently the adhesion and agglomeration of bed material. This
15 review principally examines probable mechanisms of agglomeration and the effects of operational
16 variables in reducing its severity. Additionally, an overview of monitoring and prediction of
17 agglomerate formation is given. Two key mechanisms of agglomeration are apparent in literature,
18 and both may occur concurrently dependent on fuel composition. Coating-induced agglomeration is
19 defined by the interaction of alkali metals in fuel ash with the bed material, commonly silica sand, to
20 form an alkali-silicate melt. Melt-induced agglomeration is defined by the presence of sufficient
21 amounts of both alkali compounds and silica liquid phases sourced from the fuel ash to form a
22 eutectic mixture. Physical mechanisms, such as tumble agglomeration and sintering, may further
23 enhance either of the coating-induced or melt-induced mechanisms. Of the operational variables

24 examined in this review, temperature, fluidizing gas velocity, fuel, bed material and additives have
25 been shown to have the greatest effect on agglomeration severity. Prediction of agglomeration
26 propensity may be attempted with mathematical correlations or lab-scale fuel testing before use in
27 the boiler, “pre-combustion” methods, or in-situ methods, which are focused on temperature or
28 pressure analysis. The review of the literature has highlighted the need for further research in some
29 areas, including: mechanisms when using alternate bed materials, use of dual-fuel biomass blends,
30 technical and economic optimisation of alternative bed material, the use of additives or improvers
31 and further modelling of coating growth behaviours.

32 **Keywords**

33 Fluidized bed; Combustion; Biomass; Agglomeration; Review

34 **Nomenclature**

35	AFBC		Atmospheric fluidized bed combustion
36	BFB		Bubbling fluidised bed
37	CFB		Circulating fluidised bed
38	d_{bed}	m	Bed diameter
39	DDGS		Distillers dried grain using wheat and solubles
40	FBC		Fluidized bed combustion
41	h_{bed}	m	Static bed height
42	IDT		Initial deformation temperature
43	PF		Pulverized fuel
44	PFBC		Pressurized fluidized bed combustion

45	T_{aggl}	°C	Agglomeration temperature
46	t_{def}	mins	Defluidization time
47	U	m/s	Superficial gas velocity
48	U/U_{mf}	-	Fluidization number
49	U_{mf}	m/s	Minimum fluidization velocity
50	XRD		X-Ray Diffraction

51 **1. Introduction**

52 In recent decades, there has been an increased importance placed on fuels and power generation
53 methods that emit reduced amounts of carbon dioxide (CO₂), a key contributor to anthropogenic
54 changes to the atmosphere. [1, pp. 12-19]. One fuel type that has the potential to address this issue
55 is biomass, due to its potential to approach carbon neutrality [2], and has thus been the subject of
56 research into technical issues that may negatively affects its use in the power generation industry,
57 and policy driven regulation to incentivize its deployment.

58 Biomass is a direct, low carbon alternative to fossil fuels for power and heat generation, and is
59 abundant in many areas of the world [3, 2]. In the UK it can offer competitively priced power
60 generation versus options such as nuclear and offshore wind [4]. The combustion of biomass comes
61 with several technological challenges for traditional burner technologies such as those adopted in
62 pulverized fuel (PF) power stations [5]; i.e. : low energy density after initial harvesting, variable
63 volumes of non-combustible contaminants, high moisture contents and, in most applications,
64 requires a large amounts of pre-processing/pre-treatment with specialised transportation. Due to
65 these challenges, technologies such as fluidized bed combustion (FBC) boilers have been employed.
66 FBC offers a number of advantages, such as combustion of different fuel types, blends, and ranges of
67 qualities, features commonly referred to under the umbrella term of “fuel flexibility” [5]. Hundreds

68 of full-scale bubbling fluidized bed (BFB) [6, p. 7] and circulating fluidized bed (CFB) [6, p. 8] boilers
69 have been deployed around the world [7, 8] for power generation and/or steam sales to industrial or
70 chemical plant sites. However, each FBC plant development has to overcome slagging, fouling,
71 corrosion and, most significantly, agglomeration issues resulting from the composition and
72 behaviour of the biomass fuel stock [9].

73 Analytical studies of wide ranges of fuel types have typically shown biomass to be high in volatiles
74 and moisture, with mineral matter content rich in alkali and alkali earth metals such as potassium
75 and calcium [10, 11, 12, 13]. There is also a high complexity and variation in biomass ash
76 compositions. Saidur, et al. [12] placed biomass fuels into one of three different categories based
77 upon their fuel ash composition:

- 78 • Ca- & K-rich, Si-lean. Typically woody biomass.
- 79 • Si- & Ca-rich, K-lean. Typically herbaceous or agricultural.
- 80 • Ca-, K-, & P-rich, e.g. sunflower stalk ash or rapeseed expeller ash.

81 The above components in biomass ash, together with sodium and chlorine, have been identified as
82 being responsible for agglomeration, slagging, fouling, and corrosion in Fluidized Bed boilers [10, 14,
83 pp. 471-491].

84 Agglomeration occurs within the bed itself, and is where bed particles begin to group together into
85 larger particles [14, pp. 471-491] (Figure 1). In the case of biomass combustion on a silica sand bed,
86 this is due to the formation of sticky, low melting temperature, alkali-silicate complexes. These
87 agglomerates may be further strengthened by sintering, in which high localised temperatures leads
88 to the melting of particles and thus fusing agglomerated materials into large hardened structures.
89 This method of agglomeration, in which fuel ash interacts with bed material, is typically termed
90 coating-induced agglomeration. When fuel ash contains quantities of both silica and alkali melts
91 sufficient to create melts, the term melt-induced agglomeration is commonly used. The

92 accumulation of agglomerates eventually leads to defluidization of the bed. This is the point at which
93 the bed particles no longer move and behave as a fluid in response to the fluidizing gas, as the mean
94 bed particle size will have increased and the minimum fluidization velocity, U_{mf} , is no longer achieved
95 [15].

96 In an industrial installation, operators may control agglomeration by varying fuel feeds, using
97 alternative bed materials and/or additives, moderating combustion temperatures and combustion
98 distribution, altering and moderating airflows, or varying rates of bottom ash removal and bed
99 replenishment [16, 17]. A full bed defluidization event would necessitate a plant shutdown, as the
100 bed is cooled, replenished, and started up again [18, pp. 2-110]. The financial cost associated with
101 plant outage can mean that the profitability of the plant may be at risk. Moreover, frequent start-up
102 and shutdown cycles may reduce the working lifespan of plant equipment [19, pp. 38-42]. As such,
103 considerable efforts have been made towards methods to predict or prevent agglomeration [20].

104 Considering the upper sections of the boiler, slagging on the membrane walls, fouling on
105 superheater tubes [21, pp. 406-412, 22, 23], as well as corrosion on superheater tubes [22, 24, 25,
106 26] are driven by reactions with the same chemical components as agglomeration, namely, alkali
107 and alkali earth metals, and silicon, with chlorine aiding alkali transport [27] (see Figure 2).

108 Therefore, it is important to consider the whole boiler system and the secondary or consequential
109 negative impacts when evaluating a potential mitigation or solution for any of the aforementioned
110 phenomena.

111 This review sets out to bring together the literature on the mechanisms of agglomeration, means of
112 mitigating it through varying operational conditions, and the relationships between both areas.

113 Literature from lab-scale work through to investigations on full-scale industrial boilers has been
114 selected, so that this review may be of use to both researchers and plant operators. In doing so, this
115 review has also highlighted numerous areas in which further work would be beneficial to both
116 broaden and deepen the knowledgebase.

117 **1.1 Review Scope**

118 This review focuses on the issue of agglomeration during FBC of biomass, and is divided into three
119 sections:

- 120 • A review of the mechanisms of agglomeration found within the literature
- 121 • A review of the effects of process variables on agglomeration severity
- 122 • A brief overview of the current methods to predict the occurrence of agglomeration, with
123 signposting to the other available articles and reviews on this subject

124 Summaries are provided after each section. These act to highlight key findings from the literature
125 evaluated, note the important critiques, and discuss key areas for further work noted within the
126 review. The end conclusion highlights the main areas where further work is needed.

127 **2. Mechanisms of Agglomeration**

128 As noted in the introduction, the fundamental chemistry driving agglomeration is the formation of
129 alkali silicate eutectics. This is from the interaction of SiO₂ in the bed material or ash together with
130 an alkali metal oxides in the fuel ash, such as K₂O or Na₂O. For example [28]:



132 The value of 'n' may range from 1-4. In the case of potassium silicates, higher values of 'n' generally
133 reduce the eutectic melting point: with K₂O·SiO₂ this is 976°C, whilst for K₂O·4SiO₂ the melting point
134 is 764°C [28]. These low melting points allows for the formation of a melt through the typical FBC
135 operational temperature range of 800-900°C [29], which can then cause adhesion of the bed
136 particles and agglomeration.

137 Early works into agglomeration with biomass fuels identified these eutectic melts as key drivers of
138 agglomeration [30, 31, 32]. Sintering had been identified as a key driver as agglomeration in coal
139 research [33]. Skrifvars, et al. [34] looked at this phenomena when combusting biomass, and found
140 that the presence of >15% molten phase in ash would lead to elevated amounts of sintering.

141 Skrifvars, et al. [35] then applied standardised ash testing methods to predict sintering and
142 agglomeration temperatures in biomass, to see if such methods could accurately predict
143 troublesome fuels at typical industrial operational conditions. However, there was limited success
144 with both of these methods.

145 Subsequent work on the behaviours of biomass ashes has led to the definition to two different
146 agglomeration mechanisms: coating-induced agglomeration and melt-induced agglomeration.

147 **2.1 Coating-induced Agglomeration**

148 In the work of Öhman & Nordin [36], combustion experiments for several different biomass fuels
149 were performed at lab-scale, using the “Controlled Fluidized Bed Agglomeration” methodology put
150 forth in their earlier work [37]. Here, controlled incremental heating is applied to the bed until
151 agglomeration is detected by Principal Component Analysis of temperature and pressure
152 fluctuations within the bed. This was followed by SEM/EDS analysis of the resulting agglomerates,
153 which focused on the “neck” between two joined particles.

154 The most abundant non-silica components in the agglomerates were alkali or alkaline earth metals –
155 primarily either potassium or calcium – which accounted for between 20-70wt% across the different
156 fuels. For some fuels, aluminium and iron featured amounts of up to 20wt%. Öhman & Nordin [36]
157 then proposed the following mechanism for agglomeration:

- 158 1. Ash is deposited on bed particles creating a coating, through a mixture of small particles
159 attaching to bed material, gaseous alkali molecules condensing, and reactions involving
160 gaseous alkali molecules on the surface of the bed material.
- 161 2. Sintering occurs on this bed particle coating, homogenizing and strengthening it.
- 162 3. Melting of this silicate coating layer controls adhesive forces, which influence the severity of
163 the agglomeration process. This is temperature-driven.

164 The work of Silvennoinen [38] also describes a coating mechanism similar to that of Öhman & Nordin
165 [36] and state that whilst potassium silicates are the primary chemical basis for coating layers, in
166 some cases sodium silicates are instead present. This highlights that other alkali-silicates can be the
167 basis of coating layers.

168 The works of Nuutinen, et al. [39], Visser [40], Brus, et al. [41], and Öhman, et al. [42] are closely
169 related, in that they further investigated bed particle coatings, all finding compositional and
170 structural differences through the layers, indicating the presence of multiple layers. These works
171 took samples from woody fuels, typically using quartz sand beds, at scales from lab-scale FBC units
172 to full-scale installations.

173 The presence of multiple layers appears to be a factor of the potassium content of the fuel, with an
174 example from the work of Visser [40] shown diagrammatically in Figure 3. Fuels that are lean in
175 potassium produce two layers: an “inner” homogenous layer with significant calcium content, and
176 an outer heterogeneous layer more similar in composition to that of the fuel ash. Fuel that are rich
177 in potassium produce an additional “inner-inner” layer with notable amounts of potassium. The
178 relative compositions of the inner and outer layers remain similar regardless of if the fuel is
179 potassium-rich or lean.

180 Some different observations can be seen between the works of Nuutinen, et al. [39], Visser [40],
181 Brus, et al. [41], and Öhman, et al. [42].

182 Nuutinen, et al. [39] noted that for the combustion of peat “inner” layer was absent, leaving only the
183 outer ash layer. This could perhaps be a result of the operational time, conditions, or behaviour
184 unique to peat as a fuel. Nuutinen, et al. [39] also trialled a proprietary magnesium based bed
185 particle named “GR Granule”, which had two coating layers present: an inner layer of ~60% calcium
186 and 15-20% silicon, and outer layer with notable amounts of magnesium, possibly from abrasion of
187 the bed material.

188 Visser [40] proposed a coating mechanism similar to that of Öhman & Nordin [36], albeit without
189 mention of interactions with gaseous alkali compounds. It was described as a build-up of small ash
190 particles on bed material or larger ash particles to create a coating, followed by neck formation
191 between two coated particles, which can be followed agglomeration and/or sintering. If this
192 agglomeration leads to localised defluidization, an increase in localised bed temperatures may occur,
193 triggering melt-induced agglomeration (see section 2.2).

194 Brus, et al. [41] examined agglomerate samples produced from plant-scale CFB and BFB boilers
195 ranging from 30-122MW_{th}, and those from a lab-scale BFB rig. “Inward chemical attack” by
196 potassium or calcium silicates on the original quartz sand bed particle was observed. This conclusion
197 was drawn through using quartz sand of a homogenous particle size distribution of 106-125µm,
198 taking 200 SEM images of particles before and after experimentation had occurred, and then
199 comparing the mean cross-sectional area of the sand particles before and after experimentation.
200 This is an adequate method, given the alternative of tracking and comparing a specific particle and
201 the challenges which that would entail. SEM/EDS imaging of sand particles that had been in boilers
202 for upwards of 33 days showed the diffusion of potassium into cracks in the sand particle and the
203 formation of potassium silicate veins within the sand particle. This adds additional support to the
204 conclusion of inward chemical attack occurring. Brus, et al. [41] also noted that the calcium-silicate
205 dominated “inner” coating layer is replaced by potassium- or other alkali-silicates in locations where
206 calcium is not as available, such as cracks in sand particles, or when the fuel ash contains less
207 calcium.

208 Brus, et al. [41] presented three mechanisms of agglomeration:

- 209 • Coating-induced agglomeration, with inward chemical attack by potassium/calcium silicates.
- 210 • Direct-attack by gaseous potassium compounds, forming low melting point potassium
211 silicates and resulting in viscous-flow sintering.

212 • Direct adhesion through partially melted ash derived potassium silicate particles (melt-
213 induced agglomeration, section 2.2).

214 Öhman, et al. [42] examined coating distribution across the particles examined with SEM/EDS, as
215 summarised in Table 1. To obtain their SEM/EDS data, Öhman, et al. [42] selected 3-5 particles per
216 fuel. All the fuels tested led to bed agglomeration, yet, as per Table 1, the quantity of coated
217 particles to cause agglomeration varied in from being <10% of particles examined to the “majority”,
218 which can be assumed as at least > 50%. This raises questions around the methods by which
219 agglomeration occurred: for example, whether these differences are down to sampling methods or
220 are the result of other mechanisms. Therefore, it would be worth investigating the differences
221 coating composition and frequency of coated particles across the whole bed. This may indicate if
222 certain zones are more susceptible to agglomeration and help provide a better understanding of
223 bed-scale agglomeration and defluidization mechanisms.

224 Zevenhoven-Onderwater, et al. [43] investigated the ash compositions of five different woody fuels:
225 bark, two forest residues, construction residue wood, and sawdust. From analysis of bed material
226 and fuel ash compositions, the coating layer thickness observed, and the weight of the bed before
227 and after experimentation, the source of coating elements was determined. Roughly 50wt% of
228 potassium from the fuel remained in the bed, along with 8-30wt% of the calcium and 30-65wt% of
229 fuel derived silicon, all of which could contribute to agglomeration. Coating layers were
230 homogenous, with a formation method suggested: potassium-silicates begin forming a “first layer”
231 on bed particles at around 750°C, which then captures other ash components, leading to the
232 formation of a sticky layer of melting point <800°C.

233 Grimm, et al. [44] investigated agglomeration behaviour when using Olivine as a bed material.
234 Experiments were performed for willow, logging residue, wheat straw, and distillers dried grain
235 using wheat and solubles (DDGS) fuels, on both Olivine and quartz sand beds, with a 5kW BFB

236 reactor. An Olivine bed resulted in reduced agglomeration tendency for willow and logging residue,
237 with no change noticed for wheat straw or DDGS.

238 The outer coating layer with Olivine was similar in composition to the fuel ash, as it was with quartz
239 sand. A key difference versus quartz sand though was the composition of the homogenous inner
240 coating layer for willow and logging residue, which comprised of Mg, Si and Ca as opposed to K, Si
241 and Ca. This may have been due to the methodology used: fuels were combusted at around 800°C
242 for 8 hours before the temperature was incrementally increased until agglomeration occurred or the
243 maximum of 1060°C was reached. Temperatures in excess of 1000°C, as were reached with willow
244 and logging residue, may have allowed some fraction of the magnesium in Olivine to partake in melt
245 formation. Such temperatures would not be reached in typical FBC operation, therefore this result
246 may not be wholly representative of a full-scale facility. Wheat straw and DDGS did not reach such
247 high temperatures, and did not exhibit differences in coating composition when using Olivine
248 compared to quartz sand.

249 He, et al. [45] analysed the effect of the operational time on quartz sand bed particles for a lab-scale
250 5kW_{th} BFB, 30MW_{th} BFB, and 122MW_{th} CFB. Samples were taken after the addition of a fresh bed,
251 and at intervals of several hours for the lab-scale unit or every few days for the full-scale plants. The
252 bed material was replenished at the standard operational rate for the two full-scale units: <3wt% of
253 the bed per day for the 30MW_{th} BFB unit, and 50wt% of the bed per day for the 122MW_{th} CFB unit.
254 He, et al. [45] noted similar layer composition findings to others [39, 40], though there was a time
255 dependency for their formation.

256 In the case of the 5kW_{th} BFB, a single coating layer was found on bed particles. For the 30MW_{th} BFB,
257 a single layer was found on 1 day old particles, whereas older particles displayed an inner
258 homogenous layer and outer non-homogenous layer. For the 122MW_{th} CFB, 3 day old samples
259 displayed two coating layers, equivalent in composition to the “inner-inner” and “inner” layers
260 observed by others [39, 40]. An outer layer was found only on 4 and 6 day old particles.

261 Only the 122MW_{th} CFB presented an “inner-inner” Si-K-Ca layer. The fuel used in the CFB had higher
262 ash content than the 30MW_{th} BFB (3.1wt% dry, versus 1.8wt% dry) and higher potassium content
263 (0.18wt% dry, versus 0.11wt% dry). This adds further support to the theory that an inner-inner layer
264 of Si-K-Ca is only present with sufficient availability of potassium in the fuel [39, 40].

265 Layer growth was tracked over time by He, et al. [45], the results of which are reproduced in Figure
266 4. XRD analysis on 30MW_{th} BFB samples from 3-23 days old revealed that initially K-based
267 compounds formed the majority of the mass of the layer. This then progressed to the layers
268 primarily comprising of calcium based compounds such as Ca₃Mg(SiO₄)₂, Ca₂SiO₄ and Ca₃SiO₅.

269 He et al. [45] then gave the following theory for agglomerate formation: Potassium species first react
270 with the bed particle to form low-melting point potassium-silicates. Layer growth proceeds with the
271 addition of calcium to this melt, causing precipitation of stable calcium-silicates with high melting
272 points. The increase in calcium concentration within the layer, and loss of potassium, results in a
273 weaker driving force for calcium diffusion and reaction, thus a reduced layer growth rate over time.
274 A higher amount of melt in this inner layer would influence diffusion and reaction of calcium into the
275 layer, thus influence layer growth rate.

276 Gatternig & Karl [46] have further explored coating-induced mechanisms. Experiments were first
277 performed with a progressively heated bed, and multiple coating layers were observed aligning with
278 the findings of others [39, 40].

279 Building on the inward coating growth theory suggested by Brus, et al. [41], Gatternig and Karl [46]
280 suggested that collisions between two coated particles allows for capillary action to draw coating
281 melts inwards into the particle. Additionally, from SEM/EDS imaging, visible remains of the
282 heterogeneous outer coating shell were seen in agglomerate necks/joins. Gatternig & Karl [46]
283 concluded that the outer coating layer is dry and powdery, a feature observed by others [42], and
284 that it increases in melt fraction towards the centre. On collision, this shell fractures, allowing for the
285 inner melt to form a liquid bridge, with remnants of the outer shell being present within it. Such a

286 theory diverges from previous suggestions that bridges between coated particles form during the
287 initial melt layer phase.

288 Gatternig & Karl [46] also performed experiments with a fluidized bed of sand above a fixed bed into
289 which fuel was added, to detect the effects of gaseous phase alkali compounds on agglomeration.
290 No coating layer formation was found, indicating that gaseous or aerosol alkali metals do not
291 contribute to coating formation. Others have speculated this to be the case, such as Scala & Chirone
292 [47]. However, the methodology employed by Gatternig & Karl [46] does not allow for other bed
293 phenomena to proceed, such as localised defluidization and/or bed hotspots, as there is no direct
294 contact with the fuel. However, such phenomena may provide a temperature gradient over which an
295 evaporation-condensation cycle could occur.

296 Recently, He, et al. [48] have expanded upon their previous work [45] by means of chemical
297 equilibria modelling for ash reactions and the development of a diffusion model, using the FactSage
298 software package. The data used in the model, and for validation, was that of their previous work
299 [45].

300 Temperature had a large effect on layer growth rate for operation at 850°C. The model predicted
301 layer thicknesses of 10µm at 5 days of operation and 15µm at 16 days, whilst at 900°C, a thickness of
302 about 20µm was predicted at 5 days, and 40µm at 16 days. It was suggested that the additional
303 temperature allowed for increased diffusion of Ca²⁺ into the inner melt layer, hence greater layer
304 growth.

305 The decrease in inner layer growth rate over time is suggested as being due to changes in inner layer
306 composition. Ca²⁺ diffusivity was higher in Ca₂SiO₄ than in Ca₃SiO₅, but it is the latter which increases
307 in concentration within the inner layer over time. Furthermore, the physical growth of the layer
308 would increase the diffusion distance, further impacting calcium diffusion.

309 The agglomerate coating layer growth mechanism thus suggested by He, et al. [48] is reproduced in
310 Table 2.

311 When He, et al. [48] validated the model against experimental data, the model was found to provide
312 a good indication of starting and ending coating layer thickness, though did not match the variations
313 in layer growth rate that happened on smaller timescales. This highlights an area for further work:
314 accurately modelling layer growth rate over the entirety of coating layer growth periods. This would
315 be of particular use for full-scale FBC units, as bed material is removed and replenished during
316 operation [17, 49]. The ability to accurately model and predict coating layer thicknesses across the
317 bed at any point in time could allow for optimisation of bed replenishments frequencies.

318 **2.2 Melt-induced Agglomeration**

319 Olofsson, et al. [28] proposed an agglomeration formation mechanism, “heterogeneous
320 agglomeration”, and stated that this arises due to localised “hot-spots” of over 1000°C, versus given
321 operational temperatures of ~670-870°C, allowing the creation of a melt phase of alkali-silicate
322 derived from both fuel ash and bed material. The largest agglomerates had glass-like appearance,
323 indicating prolonged exposure to high temperatures, and were 50-60mm in size, and frequently
324 caused defluidization. Olofsson, et al. [28] speculated that the causation of “hot-spots” in the bed
325 was a combination of small fuel feed fluctuations and temporary gas channelling through the bed
326 leading to localized fluidization disturbances.

327 The later work of Lin, et al. [50] presented an alternative melt-induced agglomeration mechanism,
328 from combustion of wheat straw on a quartz sand bed. After two minutes of combustion at a bed
329 temperature of 720°C, weak agglomerates were present in the form of a charred fuel pellet with
330 sand particles weakly attached. After two minutes of combustion at 920°C, the agglomerates were
331 stronger and there was far less of a char core present. After ten minutes of combustion, the char
332 core had fully combusted leaving hollow sand agglomerates in the shape of the fuel pellet.

333 Lin, et al. [50] proposed a mechanism as follows: Burning char particles had been observed as being
334 at higher temperatures than bed particles, and go from partially to almost completely molten
335 between 750-900°C. When bed particles collide with these molten char particles, they may adhere
336 to them, and become coated with the molten char melt. As the char particle burns away, the sand
337 particles would remain stuck together. Such a conclusion is supported by their results: two minutes
338 of combustion at 920°C versus 720°C resulted in a stronger agglomerate, therefore there could be
339 more of a molten char melt hence a stronger agglomerate forms. Additionally, at this temperature
340 sintering may have strengthened the agglomerate.

341 Visser [40] put forth a melt-induced agglomeration formation mechanism from a comparison
342 between a lab-scale FBC unit and an 80MW_{th} FBC plant, and described it as the result of collisions
343 between bed particles or larger ash particles, which adhere to one another due to molten ash
344 particles that function as a viscous glue. It is notable that whilst similar in nature to the method of
345 Lin, et al. [50], it does not suggest that larger molten char particles may act as a platform from which
346 agglomerates can grow.

347 Chirone, et al. [51] examined agglomeration behaviour when combusting pine seed shells, using lab-
348 scale and pilot-scale equipment. Chirone, et al. [51] proposed that bed particles stick to melting char
349 particles which then burn away, leaving behind hollow agglomerates in the shape of fuel particles.
350 Chirone, et al. [51] further suggested that combusting char particles act as a localised temperature
351 “hot-spot”. This causes more severe melting and thus more severe agglomeration than coating-
352 induced agglomerates typically display.

353 Scala & Chirone [47] studied mechanisms of agglomeration with a lab-scale unit using olive husk
354 fuel. A prior examination of the literature revealed that temperature had negligible effects on alkali
355 deposition rate, and experimentation with variable air flow rates to control temperature gave little
356 change in amounts of bed ash. Scala & Chirone [47] concluded that vaporisation and condensation
357 pathways for alkali deposition likely had a negligible effect on agglomeration. Scala & Chirone [47]

358 proposed a mechanism for agglomeration: Ash is transferred to bed particles via collisions with small
359 fine ash or large coarse char particles. Alkali species then physically diffuse through the ash and
360 interact with silica to form a eutectic. From the observations of others [50, 51], Scala and Chirone
361 [47] then stated that the transfer of alkali species by collision and their melting behaviour was likely
362 promoted by high temperature char particles. With sufficient temperature and alkali content in the
363 bed, defluidization will occur. If the bed temperature is not high enough to melt the eutectics,
364 burning char particles may provide a “hot-spot” that can drive melt formation and the accumulation
365 of smaller agglomerates, which can defluidize the bed.

366 Liu, et al. [52] looked at melt-induced phenomena, when combusting rice straw, and suggested that
367 the presence of K and Na components on the exterior of fuel fragments would allow them to form
368 adhesive alkali-silicates with relative ease. Large ash fragments ($>10\mu\text{m}$) may then bind together bed
369 material, as was evidenced by agglomerates being conjoined by necks of similar composition to that
370 of the fuel ash.

371 Gatternig & Karl [46] provided further evidence in support of the melt-induced agglomeration
372 behaviour seen by Lin et al. [50] and Chirone, et al. [51]. Gatternig & Karl [46] first observed that
373 denser fuel particles, such as wood pellets, were fully submerged in the bed during combustion thus
374 had similar temperatures to the bed itself. When testing less dense hay pellets, the pellet “floated”
375 on top of the bed and reached temperatures up to 400°C higher than the bed. This would be
376 sufficient to produce molten ash fuel pellets to drive the melt-induced agglomeration mechanisms
377 proposed by Lin, et al. [50], and may offer one explanation for temperature “hot-spots”. Gatternig &
378 Karl [46] state that lower density fuels, typically herbaceous ones, will likely undergo this behaviour.
379 This aligns with the experiences of Lin, et al. [50], whom used low density wheat straw, Chirone, et
380 al. [51] whom used pine seed shells, and Olofsson, et al. [28], whom recorded the occurrence of
381 “hot-spots” and more severe agglomeration when lower density fuels were used (sawdust, straw,
382 and meat and bone meal).

383 An aspect not explored within the literature is the relative presence of silica and alkaline metals
384 within the ash to drive melt-induced agglomerate formation. The fundamental difference seen
385 between coating-induced and melt-induced agglomeration, present throughout the literature, is that
386 the former involves the interaction of alkaline metals with silica in the bed material, whilst the latter
387 relies on the presence of both silica and alkali metals in the ash to form an alkali-silicate ash melt
388 [40, 53]. The fuels used in the majority of the works above where severe melt-induced
389 agglomeration occurred were generally herbaceous with high silica content in the ash [46, 47, 28,
390 50, 52]. Therefore, there may be a point at which the melt-induced mechanism takes precedence
391 over coating-induced agglomeration as the dominant mechanism for agglomeration, due to the
392 relative availability of silica in the ash.

393 **2.3 Physical Agglomeration Mechanisms**

394 There are several larger, bed-scale mechanisms, which may assist or propagate agglomeration.
395 These mechanisms have been explored and exploited in other industries, with comprehensive works
396 available, such as those of Pietsch [54, 55].

397 The first of these mechanisms is sintering, a mechanism frequently referenced in the literature [33,
398 36, 40, 41]. This is the process by which bridges between particles are formed or strengthened by
399 the diffusion of surface matter across particle boundaries, resulting in particles being fused together.
400 Sintering can be pressure or temperature driven, though in the context of atmospheric FBC of
401 biomass is temperature driven.

402 Tumble or growth agglomeration is a result the of sum of all forces acting to adhere the particles
403 being greater than the sum of those acting against the adhesion. The ash melts or coating layers that
404 form on or between bed particles provide an additional adhesive force between the particles, thus
405 making it easier for agglomerates to form.

406 A “molecular cramming” mechanism was first suggested by Anthony et al. [56]. It was proposed that
407 the increase in molar volume when converting calcium oxide in deposits to calcium carbonate and

408 then to calcium sulphate led to it filling any available pores or inter-particle space and produced
409 denser deposits. It was further suggested that higher quantities of materials such as iron-,
410 aluminium, and silicon-oxides in fuel ash may create small discontinuities in deposits that are
411 enhanced by molecular cramming and allow them to fracture more easily. There has been some
412 further supporting evidence for this theory [57, 58], though it appears there has been no conclusive
413 proof at the full-scale, or in the context of biomass fuels.

414 A final mechanism is pressure agglomeration [54, p. 504] whereby bonding and densification occur
415 through the application of an external force. In the context of atmospheric FBC of biomass, this may
416 occur around changes in bed geometry whereby particle can be pressed together, such as around
417 baffles or in-bed heat exchange tubes. Pressure agglomeration may also compliment tumble
418 agglomeration, as the larger agglomerates cause by the latter obstruct particle motion and cause
419 variances in pressure, allowing for pressure agglomeration to occur.

420 As can be imagined, both sintering and tumble agglomeration would enhance coating-induced and
421 melt-induced agglomeration. The larger, stronger agglomerates that result would also allow for
422 further localised temperature variation, which may allow for “hot spots” that could drive the
423 formation of larger melt fractions, further worsening agglomeration.

424 **2.4 Summary of Agglomeration Mechanisms**

425 The current knowledge of agglomeration mechanisms can be summarised as follows (shown
426 diagrammatically in Figure 7 and Figure 8):

427 **Coating-induced agglomeration (Figure 7)**

428 There is broad agreement that this mechanism is initiated via the formation of a molten adhesive
429 alkali-silicate melt upon the surface of bed particles, usually potassium-silicate, though in some cases
430 sodium-silicates if sufficient quantities are present in the fuel [38]. This layer forms via the
431 accumulation of K-compounds from fuel ash on silicate-rich bed particles, under temperatures in

432 excess of 750°C. Initial layer formation may be influenced through condensation of gaseous K-
433 species from fuel ash onto bed particles [36, 40, 43].

434 This K-silicate layer then grows inwards via reaction with silicate species in the bed material [41].
435 There may be the effects of capillary action from cracks in the bed particle drawing K-compounds
436 further inwards after collisions with other coated particles [46]. Any silica within the fuel ash may
437 also react together with potassium species on the bed material surface to generate more of a melt.
438 Calcium species from the outer ash layer begin diffusing into the molten K-silicate inner layer and
439 react to form stable species with silicate with melting points in excess of 1000°C, such as Ca_2SiO_4 and
440 Ca_3SiO_5 [45].

441 At the end of this process, bed particles typically possess two- or three-layer coatings. In the case of
442 a two-layer coating, there is an inner homogenous layer rich in Ca-silicate compounds, and an outer
443 heterogeneous layer whose composition is broadly in line with that of the fuel ash [44, 45, 46]. In
444 the case of three layer coating systems, there is an additional “inner-inner” homogenous layer, rich
445 in silicate, K, and Ca [40, 45]. The causation of this inner-inner layer has been speculated as the
446 presence of high amounts of K in the fuel [40], or perhaps the lack of diffusive driving force for Ca to
447 diffuse and react all the way to the bed particle-coating layer boundary [45, 48]. The outer ash layer
448 appears to prevent formation of further K-silicate melts, by denying K-compounds access to the
449 silicate of the bed material with which it would otherwise form a melt. In particular, magnesium in
450 the outer ash layer has been identified as preventing alkali-silicate melt formation [39].

451 Agglomeration appears to proceed at any point during layer formation. Bed particles collide, in some
452 cases breaking the outer ash layer [46], and enable that formation of a K- or Ca-silicate neck
453 conjoining bed particles [36, 40, 51]. Temperature-induced sintering may occur on the agglomerate,
454 strengthening it [36, 40, 41, 42] and with sufficient accumulation of agglomerates defluidization
455 occurs.

456 **Melt-induced agglomeration (Figure 8)**

457 The central idea of melt-induced agglomeration is the collision of larger molten ash particles with
458 bed particles, where the molten ash particles act as a viscous glue [40, 47, 51]. Scala & Chirone [47]
459 suggest that burning char particles create a localised hotspot that further enhances the adhesive
460 potential of this “viscous glue”. The resultant agglomerates are characterized by displaying a more
461 severe melting and agglomeration than traditional coating-induced agglomerates [51].

462 A notable variant to melt-induced agglomeration is when molten char particles act as a platform for
463 agglomerates to grow, as was first described by Lin, et al. [50]. Combusting char fragments have
464 elevated temperatures in comparison to the bed average, and become almost completely molten at
465 around 900°C. In collisions with bed particles, the bed particles adhere to the char fragment and the
466 viscous alkali-silicate melt on its surface. This coats the bed particles, and propagates further
467 adhesion of bed particles. Eventually, the char fragment fully combusts, typically leaving an
468 agglomerate with a hollow centre in the shape of the initial fuel fragment. The agglomerate
469 retaining the shape of the fuel particle is likely due to the ash skeleton of the fuel particle that
470 remains after combustion of the fuel pellet, a topic discussed in the work of Chirone, et al. [59]
471 (further discussed in section 3.6).

472 The elevated temperature during char combustion would allow for sintering of the agglomerate,
473 strengthening it. Gatternig & Karl [46] extended this theory, stating that less dense fuels, e.g. straws,
474 were observed to “float” on top of the fluidized bed whilst combusting, as opposed to being
475 submerged within the bed, and were exposed to higher temperatures. Moreover, Olofsson, et al.
476 [28] observed temperature hot-spots whilst utilizing less dense fuels, perhaps also due to this
477 “floating” behaviour.

478 **Recommendations for further work**

479 Agglomeration mechanisms when using non-SiO₂ based bed materials have not received a great deal
480 of work. Both Nuutinen, et al. [39] and Grimm, et al. [44] used Mg-based materials (the former a
481 proprietary material, the latter Olivine). Clearly, potassium will not react with silica in the bed

482 material to generate a K-silicate melt, yet layer formation still occurred. This is perhaps indicative of
483 a melt-induced type mechanism, though further work is needed to clarify the exact mechanisms
484 under which layer growth is occurring for non-SiO₂ based bed materials.

485 Use of chemical equilibria modelling software such as FactSage has received increased attention in
486 recent years due to improvements in the accuracy and quality of databases. The work of He, et al.
487 [48] resulted in a relatively accurate model of coating layer growth in a silica sand and wood fuel
488 scenario. However, intermediate variances and fluctuations in growth rates weren't fully captured
489 by the model, presenting an opportunity for future improvement. A more comprehensive model of
490 coating growth rate would allow for optimisation of bed replenishment in industrial facilities, and
491 allow for minimisation of agglomeration risk through prediction of the coating distribution across the
492 bed inventory. Beyond this, similar coating growth and ash melt models would be of use for
493 different fuels and alternative bed materials, again with the intention of informing agglomeration
494 risk at the industrial scale.

495 Related to this would be investigation into bed scale variances in coating composition and the
496 relative frequency and distribution of coated bed particles across the bed. If certain zones are found
497 to be particularly problematic with regards to enabling agglomeration, targeted control and
498 prevention methods may be possible.

499 Melt-induced agglomeration proceeds with sufficient silica and alkali metal content in the fuel ash.
500 However, it appears there has been no work to find a point at which the more severe melt-induced
501 agglomeration becomes the dominant form of agglomeration within the bed, due to fuel ash
502 composition. Such a value would help further inform fuel selection and fuel blending trials. Related is
503 a more general, secondary area for work, on transition points and relationships between melt-
504 induced and coating-induced agglomeration occurrence.

505 **3. Effect of Operational Variables on Agglomeration**

506 **3.1 Temperature**

507 The effects of temperature on agglomeration have been extensively researched within the
508 literature. The general trend exhibited is that with increases in temperature, there is an increase in
509 the severity of agglomeration because of the increased presence of liquid and gas phases.

510 Ultimately, this leads to a reduction in the defluidization time, t_{def} [50, 43, 60]. The elevated
511 temperatures increase the melt fraction within the ash, and decrease the viscosity of the melt [50].
512 This results in a more abundant and more mobile melt, leading to more severe agglomeration. The
513 temperatures at which FBC operate at (750-900°C) are within the range at which alkaline metal
514 complexes melt. Furthermore, the modelling efforts of He, et al. [48] highlighted that increases in
515 temperature of 50°C may lead to a 2-3x increase in coating layer growth rate. This elevated growth
516 rate would make it easier for neck formation between coated particles during collisions, due to the
517 availability of a larger melt layer, thus worsening agglomeration.

518 Conversely, lower bed temperatures delay the onset of agglomeration defluidization. For example,
519 Yu, et al. [61] found that t_{def} more than quadrupled from 60 minutes to 270 minutes by reducing the
520 operating temperature for burning straw from 800°C to 650°C. However, it is important to consider
521 that at plant scale, the end goal of combusting biomass is often to raise steam. Lowering combustion
522 temperatures will limit the conditions of the steam that can be raised, having large impacts
523 downstream of the boiler, such as on turbine efficiency [17]. Therefore, bed temperatures are likely
524 to be constrained by steam requirements.

525 **3.2 Pressure**

526 Most literature on agglomeration when using biomass utilises Atmospheric FBC (AFBC) units.
527 However, PFBC units have been seen to experience similar agglomeration phenomena to AFBC units.
528 The work of Olofsson, et al. [28] utilised a PFBC unit, showing similar phenomena to later work by

529 others who used AFBC equipment. Recent work by Zhou, et al. [62] looked at agglomeration during
530 Pressurised Fluidized Bed Gasification of biomass, which appeared to exhibit similar coating
531 phenomena to what would be experienced during AFBC of biomass. However, caution should be
532 taken when drawing comparisons between AFBC and PFBC agglomeration mechanisms, as whilst the
533 end result may be the same, the pathway there may differ.

534 **3.3 Fluidizing Gas Velocity**

535 The fluidizing gas velocity, U , has an important role to play in determining the fluidization regime in
536 any FBC system [15, 63]. Over the years, numerous researchers have looked at the effect of varying
537 U , or the ratio U/U_{mf} , known as the fluidization number, on agglomeration and defluidization.

538 Lin, et al. [50] doubled U whilst maintaining the same combustion conditions through use of N_2 . This
539 increased t_{def} by 30%. Chaivatamaset, et al. [64] found that increases to U of 28% and 60%, led to
540 average increases of t_{def} for two different fuels of 56% and 95% respectively. Lin, et al. [65] recorded
541 increases in t_{def} with successive increments in U , across four types of particle size distribution
542 (narrow, Gaussian, binary flat). Yu, et al. [61] observed reduced agglomeration by increasing U/U_{mf}
543 by a factor of 1.6, noting that agglomerates no longer presented themselves as larger clumps, but as
544 a few bed particles attached to an ash fragment.

545 It is clear then that increases in U or U/U_{mf} will cause an increase in t_{def} . With increases in U , bed
546 particles gain momentum thus are more likely to overcome adhesive forces during collisions with
547 coated bed particles and molten ash particles [50, 65]. Furthermore, higher U values would lead to
548 more vigorous bed mixing. This in turn would reduce the chance of certain areas experiencing poor
549 fluidization; a behaviour suspected to propagate agglomeration.

550 **3.4 Gas Distribution Uniformity**

551 An aspect that has received little direct investigation is that of the fluidizing gas distribution
552 uniformity on agglomeration. Bubbles will form at the bottom of the fluidized bed as gas is released

553 from the gas distribution plate. These bubbles will coalesce into larger ones as they rise through the
554 bed [15]. This bubble movement drives fluidisation and heat transfer within the bed, as well as how
555 well mixed it is [66], thus if impaired may have significant effects on operation.

556 Oka [67] suggests that with damaged bubble cap, thermal diffusivity across the bed would be
557 reduced and the bed hydrodynamics would be altered. This would create regions of high and low
558 turbulence, and lead to temperature gradients across the bed that may assist or accelerate the
559 formation of agglomerates. Kuo, et al. [68] trialled a fixed grate furnace with wood fuel, and gave a
560 comparison between sidewall air injection and under-grate air injection. They noted that changing
561 the air distributor configuration had significant effects on flame coverage, and led to higher and
562 lower temperature regions within the furnace. This behaviour could increase the rate of
563 agglomerate formation. Lin, et al. [65] found that a temporary burst of high velocity air was
564 sufficient to break apart in-situ agglomerates and postpone a defluidization event. This could imply
565 that a region of higher turbulence in the bed may be beneficial for minimising agglomerate
566 formation.

567 The work of Chilton [69, pp. 225-291] aimed to test the effects of non-uniform air distribution when
568 using five different biomasses in a 200kW_{th} FBC unit. A uniform air distributor with 30 evenly spaced
569 bubble caps was compared against with one that had 18 slightly larger bubble caps plus an ash chute
570 occupying one corner of the distributor. The ash chute had an air gap around it, allowing for air
571 leakage and further non-uniformity. Use of the non-uniform plate created greater variations in
572 temperatures across the bed and freeboard, and in emissions. Data on defluidization times was less
573 conclusive. Peanuts and straw experienced reductions in defluidization time of 10% and 40%
574 respectively with the non-uniform air distribution plate, whilst oats experienced an increase of 181%
575 and miscanthus an increase of 73%. Whilst this does not provide a conclusive result on the effects of
576 gas distribution uniformity on agglomeration, it does indicate that differences in distribution plate

577 design, and the effects of bubble cap failures or leaks, can be significant on defluidization times. It
578 also shows that it is an area where future work may be useful, albeit challenging to execute.

579 **3.5 Static Bed Height**

580 Lin & Wey [53] examined the effects of static bed height on t_{def} during FBC of waste. Increases in the
581 Bed Height to Diameter ratio (h_{bed}/d_{bed}), produced a non-linear decline in t_{def} (Figure 9). The
582 explanation cited was reduced vertical mixing with increasing bed height, allowing for agglomeration
583 to proceed more easily upon release of alkali-metals from ash. However, a reasoning was not
584 proposed for the rate of this decline, in particular from $2.0h_{bed}/d_{bed}$ and $2.3h_{bed}/d_{bed}$. This is perhaps
585 indicative of some larger change in the bed dynamics when moving between these two bed heights,
586 thus allowing for defluidization to occur much sooner. However, this was not explored further.
587 Moreover, the timescales of t_{def} are all below 15 minutes, meaning that smaller irregularities e.g. in
588 fuel feeding, may have a large proportional impact on the results.

589 Chaivatamaset, et al. [64] examined the effect of static bed height on t_{def} , and observed behaviours
590 that were opposite to those noted by Lin & Wey [53]. Doubling h_{bed} whilst maintaining the same
591 fluidizing gas velocity, temperature and bed particle size resulted in increases in t_{def} of between 5-
592 55%, dependent upon the fuel and fluidizing velocity. Corncob typically showed greater percentage
593 increases than Palm Shell in response to increases in static bed height. No further comparison was
594 performed between agglomerates from the two different static bed heights examined.

595 It may be of interest to further examine the effects of static bed height on agglomeration, t_{def} , and
596 determining any relationships that may exist. A larger static bed height is known to allow the
597 coalescence of bubbles to larger sizes, and causes increased turbulence at the top of the bed [70].
598 This behaviour may also influence that seen through the observations of Gatternig & Karl [46],
599 whom noted that low density fuel pellets floating on the bed surface caused severe melt-induced
600 agglomeration. Therefore, the effects on agglomeration of bubble size and behaviour at the bed
601 surface may be worthy of investigation.

602 **3.6 Fuel**

603 **Fuel Type**

604 The effects of different fuels on agglomeration have been extensively researched. As noted in the
605 introduction, fuel and ash composition can vary massively across different biomass fuels [10, 11]. As
606 illustrated in section 2, the presence of alkali and alkali earth metals within fuel ash is a key
607 contributing factor to agglomeration severity.

608 Works such as those by Skrifvars, et al. [34], Öhman, et al. [36], and Brus, et al. [41], have looked at
609 fuels across a variety of different biomass categories. Fuels with high amounts of alkali metals within
610 their ash agglomerate more quickly, and at lower temperatures. For example, fuels such as straws
611 are particularly bad due to their high potassium contents, as discussed by Yu, et al. [61]. As a general
612 comment, fuels with a combination of high silica content and high alkali content, such as straws,
613 seem predisposed to agglomerating via melt-induced agglomeration, as the fuel ash itself has the
614 necessary material to create an alkali silicate melt. In industrial and plant-scale settings, woody fuels
615 have emerged as the preferred fuel type for FBC of biomass, due to their less severe agglomeration
616 tendencies [17].

617 **Co-firing**

618 Co-firing of biomass fuel blends may be performed due to economic and operational needs, for
619 example balancing usage of a better quality, more expensive fuel with a poorer, cheaper one [71, 72,
620 17]. Whilst there is a sizable body of research available on co-firing of coal-biomass blends, there are
621 fewer systematic studies available on biomass fuel blends and the effects of altering blend ratios.
622 Hupa [71] notes that there was an increasing number of FBC boilers employing co-firing in the 2001-
623 2002 period, some of which using biomass-only fuel blends, and this amount would likely have only
624 increased with time as there are more FBC units online thus greater competition for biomass fuels. A
625 recent review on biomass combustion and ash behaviours by Hupa [73] again notes the lack of
626 knowledge surrounding co-firing of biomass blends.

627 Salour, et al. [74] blended rice straw with wood, in order to control the severe agglomeration
628 ordinarily caused by rice straw. When combusted at a bed temperature at or below 800°C, blends of
629 up to 50% rice straw were acceptable. Beyond this, t_{def} decreased with increasing rice straw fraction.
630 Salour, et al. [74] also measured key ash fusion temperatures such as the initial deformation
631 temperature (IDT). These were found to be non-linear in behaviour, Figure 10 providing an example.
632 Non-linear behaviours such as these add difficulty in predicting the behaviour of fuel blends, and
633 highlight the need further systematic studies of behaviour with blend variations.

634 Davidsson, et al. [75] examined the effects of biomass co-firing in a 12MW_{th} CFB with a mixture of
635 86% wood and 14% straw pellets on an energy basis. This produced a high level of alkali deposits
636 compared to their coal based tests, a result of alkali metal content in the straw. Concentrations of
637 KCl in the flue gas rose from around 3-4ppm with wood pellets to 20ppm with the 14% straw blend.

638 Thy, et al. [76] investigated agglomeration behaviour of a blend of wood with between 2.6-25.0wt%
639 rice straw. They found a strong positive correlation between increasing amount of straw and
640 severity of agglomeration, with blends of 2.6wt% rice straw producing mild agglomeration whilst
641 those of 9.6% and above resulted in defluidization and large plugs of agglomerates being extracted.
642 A visual estimation of the proportion of the bed that suffered from agglomeration produced an
643 exponential relationship between percentage agglomerated and percentage rice straw content.

644 Elled, et al. [77] explored usage of a wood-straw fuel blend. A two layer coating was formed on bed
645 particles, the inner layer dominated by potassium silicates, whilst the outer layer comprised
646 primarily of calcium silicates. Whilst these results broadly align with what is typically seen in a single
647 fuel system, a closer comparison was not drawn.

648 Silvennoinen & Hedman [78] examined the effects of co-firing wood biomass with up to 30wt%
649 sunflower seed hull pellets or oat seeds, in a 75MW_{th} commercial BFB. During their experimentation,
650 no agglomeration was detected, a result of an intentional reduction of temperature to 750°C which
651 would bring the system to just above the melting point of potassium-silicate eutectics (742°C).

652 Becidan, et al. [79] modelled the effects of a binary system consisting of straw with either peat or
653 sewage sludge on alkali chloride formation; a key driver of corrosion [25, 26]. Non-linear
654 relationships were exhibited with increasing weight percentages of peat or sewage sludge, and the
655 mechanisms and elements affecting formation and decomposition of alkali chlorides changed with
656 fuel blend ratios. This further highlights the complexities of using biomass fuel blends.

657 The works of Suheri & Kuprianov [80] and Sirisomboon & Kuprianov [81] looked at varying blend
658 ratios of binary biomass mixtures, as well as combustion excess air ratios, on emissions and
659 combustion efficiency. Emissions behaviours here seemed to scale more proportionately between
660 varying secondary fuel percentages.

661 **Fuel Particle Size**

662 Lin, et al. [50] performed an experimental run with smashed straw pellets of particle size <1mm, to
663 compare against straw pellets of sizes 1-10mm, but did not find a notable change in t_{def} . The work of
664 Yu, et al. [61] looked at the effect of straw fuel size, with a comparison of small straw bales against
665 milled straw powder, in a lab-scale BFB. Use of the powder allowed for a total fuel feeding of 281g,
666 as opposed to 110g for the bales. However, the low density of straw powder may allow for it to be
667 easily entrained within the flue gas. An analysis of the amount of unburnt carbon within the fly ash
668 in not provided, nor an analysis of the potassium retained within the bed at the end of the run.

669 Therefore, it cannot be stated if this elevated level of fuel feeding before defluidization is simply due
670 to fuel becoming entrained within the flue gas.

671 Burton & Wei [82] looked at the effect of fuel particle size in the context of Fluidised Bed Pyrolysis. A
672 relation between biomass fuel particle size and 'Sand Loading' was drawn; this latter term being
673 defined as the mass of bed sand adhered to fuel particles normalised against the total mass of fuel
674 fed. Sand Loading increased with fuel particle size up to 430 μ m, and then decreased until reaching a
675 plateau at around 1500 μ m. This was suggested as being due to transfer of the sticky alkali coating

676 within the fuel particle being convection controlled to a particle size of 430 μ m, and diffusion
677 controlled at larger sizes.

678 Also related are the combustion profiles of a fuel. Chirone, et al. [59] performed a comprehensive
679 investigation into combustion profiles and characteristics of three pelletized fuels: wood, straw, and
680 sludge. Fuels underwent several repetitions of a combustion-quenching process, in order to examine
681 the condition and structure of fuel pellets at successive times. With sludge a “shrinking core” pattern
682 was seen, where the initial size of the pellet was preserved with an ash skeleton that remained after
683 burn-off of the carbon. Wood followed a “shrinking particle” pattern, whereby the pellet slowly
684 shrank and fragmented over time. Straw took a pathway almost between these two. Shrinkage of
685 the pellet was observed, but an ash skeleton did remain, and said skeleton had bed sand adhered to
686 it. This ash skeleton supports the melt-induced agglomeration observations of Lin, et al. [50] and
687 Chirone, et al. [51] whereby an agglomerate is formed in the shaped of a fuel particle (section 2.2).

688 **Fuel Moisture**

689 Fuel moisture has not been investigated in relation to agglomeration behaviour in the literature. This
690 may be of interest due to the high relatively moisture content of biomass fuels, e.g. wood has been
691 reported as having a moisture content of 40-70% [27]. This moisture content affects parameters
692 such as the fuel heating value, bed temperatures, and flue gas composition during combustion [10,
693 27]. Higher moisture content negatively affects the overall boiler efficiency, as additional heat
694 energy is used on the fuel drying phase of combustion, and larger variations in moisture content will
695 affect combustion control [83]. However, it is known that water will leach out soluble fractions alkali
696 and alkali earth metals responsible agglomeration problems [11], thus there is some benefit in the
697 fuel initially being exposed to a higher moisture content.

698 **Fuel Feeding Rate**

699 Fuel feeding rate has not been directly investigated as a factor, largely because a higher fuel feeding
700 rate for a FBC unit would imply a higher thermal rating. Therefore, higher temperatures will naturally
701 result, the effects of which are described in section 3.1. Moreover, it will of course provide more fuel
702 ash to drive agglomeration.

703 **3.7 Bed Material**

704 As is evident throughout section 2, the common denominator for agglomeration is the presence of
705 large quantities of silica within the bed material. Thus, research has been ongoing for alternative bed
706 materials. A selection of these results have been summarised in Table 3.

707 Substituting SiO₂-based sands for materials dominant in Mg, Al or Ca has a proven positive effect on
708 reducing agglomeration, as doing so reduces or eliminates the availability of silicon for
709 agglomeration. The exception is for fuels that contain sufficient amounts of Si to drive the formation
710 of alkali-silicate melts themselves, such as straw, as seen in several works [44, 75, 61]. Use of
711 different bed materials does still have some positive effect on lengthening t_{def} in these cases though.
712 More recently, Knutsson, et al. [84] investigated the potential of mixing bed materials to balance
713 performance and economic aspects, an idea little explored in the literature. Varying mixtures of one
714 to all of silica sand, bauxite (Al₂O₃), K₂CO₃, and CaCO₃, were thermodynamically modelled and tested
715 experimentally. The presence of bauxite with silica sand or K₂CO₃ weakened agglomeration tendency
716 over silica sand alone, as did blends with CaCO₃, which had a stronger effect on reducing
717 agglomeration tendency. Knutsson, et al. [84] state that calcium forms a barrier preventing further
718 diffusion of potassium into silicate melts. This appears to be an exploitation of the protective
719 capabilities of calcium described by He, et al. [45], by forming a calcium-silicate protective layer
720 faster than one would otherwise arise during the natural progression of coating-induced
721 agglomeration.

722 Corcoran, et al. [85] trialled a blend of quartz sand with up to 40wt% Ilmenite (FeTiO₃) when
723 combusting wood. It was found that a very thin layer of potassium from fuel ash would initially form

724 on the Ilmenite, and this would disappear as the potassium diffused into the bed particle, thus
725 removing its availability for driving agglomeration and corrosion. Iron was found to migrate
726 outwards to the surface of the Ilmenite bed particle, and calcium from fuel as was observed to form
727 a layer on the surface of the Ilmenite particle. This may have prevented further diffusion of
728 potassium inwards, similar to the calcium observations of Knutsson, et al. [84] and He, et al. [45].
729 Recently, energy supplier E.ON has begun using an Ilmenite-based bed material named “Improbed”
730 in several of their FBC units [86].

731 **3.8 Bed Material Particle Size**

732 Figure 11 provides graphs of the effect of changing average bed particle size on t_{def} from four
733 separate works. The trend exhibited is that with an increase in bed particle size, there is a reduction
734 in t_{def} . Some notes on these graphs are as follows:

- 735 • Lin, et al. [50] maintained a constant temperature and superficial gas velocity, U , between
736 the two d_p values. They suggested that poorer mixing due to the smaller U/U_{mf} ratio for the
737 larger particles led to a lower t_{def} .
- 738 • Chaivatamaset, et al. [64] also maintained a constant fluidizing gas velocity across the bed
739 particle sizes. Tests for all fuels at 900°C also showed decreases in t_{def} with increases in d_p .
- 740 • Yu, et al. [61] used a near constant U/U_{mf} value for all three particle sizes, as opposed to
741 maintaining a constant U value as Lin, et al. [50] and Chaivatamaset, et al. [64] did. However,
742 Yu, et al. [61] also hand fed bundles of straw every 20 seconds as fuel. This non-continuous
743 fuel feeding method have affected results somewhat.
- 744 • Lin & Wey [53] combusted Municipal Solid Waste (MSW) within a Fluidized Bed, a fuel with
745 similar agglomeration characterisations to biomass due to its high Na content. They note
746 that sand particles up to 770 μm acted as a Geldart Group B powder, whilst the 920 μm sand

747 acted as a Group D powder. This change in Geldart classification is accompanied by a sharp
748 decline in t_{def} .

749 The distinction between the Geldart particle classifications by Lin & Wey [53] is perhaps an
750 important one: particles in Group B favour bubbling behaviour at U_{mf} , whilst Group D will spout as
751 they more readily form large bubbles [87, 15]. This raises the question of the potential impact of
752 different Geldart powder classifications on agglomeration during FBC of biomass, and if a wider
753 study may reveal relationships between particle size, Geldart particle classification, and
754 agglomeration. For example, perhaps the bubbling behaviour of Group B acts to minimize the
755 formation of potential agglomerates by improved bed mixing, whereas Group D materials may allow
756 for bed material to end up grouped together, promoting temperature non-uniformities and
757 agglomerate formation.

758 Scala & Chirone [60] reported a different trend for increases in d_p (Table 4). Increases in d_p by a
759 factor of 2-3 led to an approximate doubling of t_{def} for all fuels and scenarios. In the Pine Seed Shells
760 data fuel feed rate was reduced to increase amounts of excess air which may explain increases in
761 t_{def} . However, this was not the case for the virgin olive husk fuel, which exhibited the same trend.
762 The reasoning for this put forth by Scala & Chirone [60] was that large particles will participate in
763 more energetic collisions, making it harder for adhesive forces to mitigate these and cause adhesion
764 between the particles.

765 Lin, et al. [65] performed a comprehensive study on the effects of different d_p distributions of sand
766 on t_{def} , albeit for MSW as opposed to biomass. Four d_p distributions were selected:

- 767 • A narrow distribution of d_p between 590-840 μm
- 768 • A Gaussian distribution where d_p ranged between 350-1190 μm
- 769 • A Binary distribution where 59% of bed mass was 840-1000 μm , whilst the remainder was
770 500-590 μm

- 771 • A flat distribution, ranging between 350-1190 μm

772 Increases in fluidizing gas velocity resulted in larger values of t_{def} across the board. The narrow
773 distribution showed a noticeably longer t_{def} , sometimes up to 20% longer than the other
774 distributions at 700°C and 800°C. The Gaussian distribution also showed slightly longer t_{def} compared
775 to the other two distributions. At 900°C however, there was almost no difference in t_{def} between the
776 distributions, perhaps indicating severe ash melting due to the temperature. With increasing Na
777 concentration in the bed, t_{def} declined as would be expected, but the narrow distribution frequently
778 produced the largest values of t_{def} , with the Gaussian distribution also showing slightly higher values
779 of t_{def} . At the highest Na concentration, there was little difference between the four distributions.

780 The work of Lin, et al. [65] indicates the potential importance of particle size distribution. The
781 narrow distribution displayed some sizable increases in t_{def} over the other distributions at moderate
782 temperatures and sodium contents, a behaviour displayed to a lesser extent by the Gaussian
783 distribution. However, different distributions of smaller particles were not examined here, and these
784 were seen to produce longer t_{def} times in the work of others [50, 64, 61]. Therefore, further work
785 into finding the optimal particle size distribution for typical bed materials may be worthy of
786 investigation.

787 **3.9 Additives**

788 The use of additives to minimize or eliminate agglomeration has been a key area of research. The
789 work of Steenari & Lindqvist [88] identified Kaolin and Dolomite as increasing the ash melting
790 temperature for straw ash, with the former having a greater effect. Öhman & Nordin [89] trialled
791 Kaolin, comprising primarily of Kaolinite ($\text{Al}_2\text{Si}_2\text{O}_5(\text{OH})_4$) with some Halloysite ($\text{Al}_2\text{Si}_2\text{O}_5(\text{OH})_4(\text{H}_2\text{O})_2$).
792 An amount of 10wt% of a quartz bed sand bed was used, with bark and wheat straw as fuel. For
793 wheat straw the agglomeration temperature, T_{aggl} , increased from 739°C to 886°C, whilst for bark it
794 increased from 988°C to 1000°C. The Kaolin used had transformed into meta-kaolinite and absorbed
795 potassium, thus denying potassium for agglomeration.

796 Olofsson, et al. [28] experimented with the addition of mullite, calcite, clay, and a clay-calcite
797 mixture, each 10wt% of the bed, for different bed materials and fuels. Mullite was found to largely
798 mitigate agglomeration, clay worsened agglomeration due to its potassium content of 1.28wt%,
799 whilst calcite was present in agglomerates but had a somewhat positive effect on reducing
800 agglomeration severity.

801 Davidsson, et al. [72] trialled several additives in a 12MW CFB for the combustion of a blend of wood
802 pellets and straw pellets on a quartz sand bed. When using Kaolin as an additive, T_{aggl} of cyclone ash
803 samples were over 100°C above those of samples where Kaolin wasn't used. A molar ratio of Kaolin
804 to alkali of 0.85 was sufficient to maintain a $T_{\text{aggl}} > 1100^{\circ}\text{C}$. The effects of ammonium sulphate and
805 sulphur were also monitored. These additives are typically used for corrosion control [25, 26]. In
806 theory, these would convert gaseous KCl into K-sulphates, and favour the release of potassium into
807 the gaseous form. Ammonium sulphate gave a small increase in T_{aggl} of around 50°C to 919°C, whilst
808 sulphur had no such effect.

809 Vamvuka, et al. [90] tested Kaolinite ($\text{Al}_2\text{Si}_2\text{O}_5(\text{OH})_4$), Clinoclone ($(\text{Mg,Al,Fe})_6[(\text{Si,Al})_4\text{O}_{10}](\text{OH})_8$) and
810 Ankerite ($\text{Ca}(\text{Mg,Fe,Mn})(\text{CO}_3)_2$) for the combustion of olive kernel and olive tree wood on a Na-
811 feldspar bed. The authors state that this bed material was selected itself to reduce agglomeration,
812 thus will affect the apparent effectiveness of these additives. All three additives prevented
813 agglomeration during the tests, retaining alkali species within the bottom ash.

814 Zabetta, et al. [17] discuss the commercial experiences of Foster Wheeler with additives. They too
815 note that Kaolin has been found to be the most effective, but also list some alternatives used with
816 their boilers such as bauxite, emalthisite, sillimanite, and diatomaceous earth. These materials are
817 noted to contain one or more of silicon-, aluminium-, or iron-oxide which react with H_2O to form HCl,
818 transferring the alkali to the mineral used and preventing the formation of KCl.

819 Lin, et al. [91] investigated the addition of calcium and magnesium for incineration of waste. Both
820 reduced agglomeration tendency and increased t_{def} , when the molar ratio of Na, which drove

821 agglomeration in waste incineration, to Mg or Ca was below 2. Above this ratio there was no
822 inhibiting effect.

823 To summarise, additives that are rich in Mg, Ca, or Al have a positive effect in reducing
824 agglomeration tendency, similar to use of alternative bed materials (section 3.7); Kaolin in particular
825 has been successful. Moreover, additives generally retain alkali species within the bottom ash, thus
826 preventing it from contributing to fouling, slagging or corrosion. Agglomeration may still proceed for
827 fuels that produce melt-induced agglomeration, though additives still have a positive effect. It would
828 perhaps be of some interest to investigate the effects of varying additive dosage, relative to the
829 molar amount needed for the fuel feed rate. This could help determine the relative technical
830 benefits of under and overdosing additives on both bed agglomeration and other downstream issues
831 such as slagging, fouling and corrosion.

832 **3.10 Effect of Additives and Alternative Bed Materials on Chlorine Emissions**

833 As discussed in sections 3.7 and 3.9, additives and alternative bed materials will alter or prevent the
834 reactions that would otherwise occur between bed material and fuel ash. The behaviour of Chlorine
835 may be of particular interest, as it acts as an alkali carrier gas driving fouling, slagging, and corrosion
836 [21, 22, 23, 24, 25, 26].

837 Coda, et al. [92] trialled use of Kaolin, Bauxite, and Limestone as additives with wood and waste
838 fuels. Kaolin doses of 25% mass of fuel ash had little effect on Cl in flue gas, whilst moving Kaolin
839 dosage to 50% mass of fuel ash almost doubled the Cl content in flue gas, a value that remained near
840 constant when further increasing Kaolin dosage to 79% mass of fuel ash. Bauxite had a similar effect,
841 whereby a dosage of 40% mass of fuel ash gave a 100% increase in Cl in the flue gas. This emphasises
842 the large effect that additive dosing can have on emissions.

843 Davidsson, et al. [72] attained some emissions data when using Kaolin as an additive or Olivine as a
844 bed material in a 12MW_{th} CFB combusting a blend of wood and straw. Three different Kaolin doses
845 were trialled, leading to increases of up to 50% in HCl concentration prior to the convective pass,

846 over reference values of 55-60ppm. Sharp declines in alkali chloride concentrations were observed,
847 as would be expected, due to the reaction of the Kaolin with alkali metals in fuel ash. At the stack
848 HCl concentrations were doubled with high Kaolin doses compared to those without Kaolin. These
849 increases in HCl concentration, particularly at the stack, should be noted in regards to what the
850 allowable metal losses due to HCl corrosion are.

851 Use of Olivine instead of quartz sand as a bed material caused alkali chloride concentrations in the
852 convective pass to almost double. HCl concentrations here were also higher by around 30%.

853 Downstream at the stack, HCl concentrations were approximately 30% lower with Olivine. The
854 Olivine does not contain significant quantities of silica thus would not react with the alkali metal
855 content of the fuel, hence allowing it to form alkali chlorides instead. Once again, these elevated
856 quantities of HCl and alkali chlorides would be of concern when considering the acceptable metal
857 losses due to corrosion.

858 These findings reinforce the idea that the boiler system must be considered as a whole, since
859 solutions to one issue may free up additional material to drive another. It also highlights that there
860 would be value in a comprehensive study that evaluates the effects on the whole boiler system
861 when using additives or alternative bed materials. For example, ammonium sulphate is a common
862 additive used to convert alkali chlorides into alkali sulphates [26], though if used in a system with an
863 Olivine bed there would be significantly more alkali chlorides available, thus the potential for
864 elevated HCl concentrations given sufficient amounts of ammonium sulphate.

865 **3.11 Coating Thickness**

866 The idea of a “Critical Coating Thickness” and the effects of liquid layering on particles in a fluidised
867 bed is one that been discussed in the literature for many years. For example, Seville & Clift [93]
868 noted that the continuous addition of liquid layers to fluidised particles of Geldart Group B would
869 cause them to transition to Geldart Groups A and C, as inter-particle forces are enhanced. A “Critical
870 Coating Thickness” would be the point at which neck formation between coated particles occurs and

871 bed agglomeration proceeds. Brus, et al. [94] performed an analysis of coating thickness over time,
872 taking samples from industrial scale FBC plants, and stated that the critical coating thickness is less
873 than 10 μ m. The recent work of He, et al. [45] provides a systematic investigation into coating
874 thickness over time for a lab-scale BFB, 30MW_{th} BFB, and 122MW_{th} CFB. An initial rapid growth of
875 coating layers occurred over the first several days in the full-scale units. This growth rate declined as
876 diffusion of calcium into the melt began and higher melting point calcium compounds formed.
877 However, there was no further discussion of a critical coating thickness. Others in the literature have
878 also mentioned the idea of a critical coating thickness with little other discussion [39, 43, 47, 95].

879 **3.12 Size & Scale of Fluidized Bed**

880 For generating solutions to industrial problems at the lab- or pilot-scale, it is important to
881 understand the applicability of results and findings to full-scale FBC plants. Many researchers have
882 investigated agglomeration in full-scale plants, and performed direct comparisons to samples
883 produced by lab- or pilot-scale facilities. Visser [40] looked at agglomerates from both the lab-scale
884 and the 80MW_{th} Cuijk FBC unit in the Netherlands. The two operational differences between these
885 setups were that the lab-scale unit had fuel fed directly into the bed, whilst for Cuijk it was above-
886 bed, and that there was a constant bed renewal and replenishment cycle in effect at Cuijk. This
887 bottom ash removal and bed replenishment ability is a common agglomeration control strategy
888 within industry [17, 49]. However, it is also one not available to most lab- and pilot-scale facilities. It
889 is of note that variations to replenishment rate to determine the effect on agglomeration is not
890 something that appears to have been examined in the literature, but equally would require a
891 suitable lab- or pilot-scale facility.

892 Visser [40] concluded that lab-scale agglomeration testing provided a representative view of the
893 initial stages of plant-scale agglomeration. The constant replenishment of sand at the Cuijk bio-
894 energy plant was believed to be the cause of some of the differences in the chemistry of outer
895 coating layers, due to providing fresh material for chemical reactions. Furthermore, samples at Cuijk

896 had thicker coatings due to a longer average residence time in the bed compared to the lab-scale
897 agglomerate samples.

898 Others have also observed consistent results between lab- and full-scale facilities, be it for topics
899 such as agglomeration mechanisms, additives, or fuels, albeit with the same shortcomings such as
900 those seen by Visser [40], e.g. thinner coatings due to shorter residence times [38, 39, 45, 72, 78].

901 One difference suggested by Chirone, et al. [51] is that a pilot-scale fluidized bed provided a longer
902 t_{def} time compared to a lab-scale setup due to higher inertial forces in the bed. A comparison
903 between a pilot- and lab-scale unit resulted in a t_{def} that was 3.6 times longer at pilot-scale, and had
904 a higher ash content within the bed at time of defluidization (4wt% versus 2wt%). Chirone, et al. [51]
905 suggested an increase in inertial forces inside the bed when moving up in scale would counteract the
906 formation of weaker agglomerates that might otherwise cause a quicker onset of defluidization.
907 Therefore, at plant-scale higher inertial forces may also assist in lengthening t_{def} .

908 **3.13 Summary of Effects of Operational Variables**

909 Table 5 summarises the effect of operational variables on agglomeration.

910 Increases in combustion temperature have a sizable effect on agglomeration, by increasing the
911 amount of alkali-silicate melt that is generated and making it less viscous. Therefore a lower
912 temperature is desirable, insofar as it does not have too great of an impact on the conditions of
913 raised steam at full scale.

914 From the limited literature available on agglomeration in PFBC units, the final agglomerates formed
915 in PFBC units seem of similar composition and type to those that would form in an AFBC.

916 Increases in the fluidizing gas velocity, U , have consistently produced longer values of t_{def} in the
917 literature. This appears to be a result of two factors:

- 918 • Better in-bed mixing preventing the formation of localized temperature hot spots or bed
919 dead-zones.

920 • Higher kinetic forces of bed particles that may overcome adhesive coating or melt forces.

921 There is little research on the effects of static bed height, and what is available is not conclusive.

922 Work using a constant U value across several bed heights has produced an increase and decrease in

923 t_{def} with increasing bed height, indicating perhaps the involvement of other factors. Additionally,

924 increases in bed height allow for coalescence of bubbles to larger sizes. Therefore, will be increased

925 turbulence at the bed surface where the bubbles exit, which in turn may affect combustion

926 behaviour of the fuel particles and agglomeration behaviour.

927 Investigations into bed material particle size have generally shown that increasing d_p , even whilst

928 maintaining a constant U/U_{mf} , leads to a reduction in t_{def} thus worsened agglomeration. Variations of

929 bed particle size distribution for larger bed particles have shown that Gaussian and narrow

930 distributions provide longer t_{def} values.

931 Alternative bed materials that comprise primarily of aluminium-, calcium-, or magnesium-oxides, as

932 opposed to the SiO_2 , have been shown to reduce or eliminate agglomeration. A change of the bed

933 material can increase the ash fusion temperature of complexes forming, and in doing so reduce melt

934 phases. The exception is where a fuel is rich in both alkali metals and SiO_2 , such as straw, which will

935 form a melt-induced agglomerates with just its fuel ash contents.

936 Similar to bed materials, aluminous-, calcium-, or magnesium-based additives have been shown to

937 be effective. Kaolin in particular has shown itself to be successful in reducing or eliminating

938 agglomeration several times within the literature. Both additives and bed materials have been noted

939 to have a large effect on emissions, particularly Chlorine, which can drive corrosion mechanisms.

940 Fuel has a large influence on agglomeration. Fuels with increasing amounts of alkali metals such as

941 potassium exhibit more severe agglomeration, typically melt-induced agglomeration, and lower

942 values of t_{def} . Co-firing of fuels is something primarily explored in the context of coal-biomass or

943 wood-straw mixtures within the literature. A common trend for biomass blends is that relationships

944 between blend ratios and agglomeration factors such as melt temperatures are non-linear. Fuel
945 particle size has receive some attention, with smaller particle sizes giving better combustion
946 efficiencies and longer values of t_{def} . This is perhaps due to combustion taking place at higher regions
947 of, or just above, the bed.

948 Coating thickness and critical values for triggering agglomeration are of general interest. Growth
949 rates are typically quicker at the start and then trail off due to diffusion of Ca into the K-silicate melt,
950 forming a Ca-silicate melt of higher melting point. Neck formation between coated particles can
951 occur at coating thicknesses less than 10 μ m.

952 The applicability of lab- and pilot-scale results to full-scale facilities has been explored within the
953 literature. Mechanisms and behaviours generally map well to full-scale facilities for the initial
954 triggering of agglomeration. Over time, there is a divergence due to replenishment of bed material
955 in full-scale facilities, plus longer residence times, leading to thicker coatings on bed particles.

956 **Recommendations for further work**

- 957 • Large bed heights allow for further coalescence of bubbles, leading to greater turbulence at
958 the surface of the bed, as well as enhanced combustion efficiencies [6, 70]. Gatternig, et al.
959 [46] observed that less dense fuel particles “floated” on the surface of the bed, reaching
960 higher temperatures, and exacerbating agglomeration issues, thus there may be interest in
961 the effects of bed height on agglomeration severity.
- 962 • Smaller particle sizes have generally been shown to lengthen t_{def} , and certain particle size
963 distributions (Gaussian, narrow) have been shown to lengthen t_{def} albeit with larger average
964 particle sizes. Therefore, it would be of interest to trial different size distributions of a
965 smaller mean particle size, to see if similar findings are apparent, and if there may be an
966 optimum size range and size distribution.
- 967 • Several alternative bed materials and additives have been shown to mitigate or prevent
968 agglomeration in numerous studies, with some such as Olivine (bed material) and Kaolin

969 (additive) being used in industrial installations. Investigatory work into new bed material and
970 additives would always be welcomed, but also more comprehensive studies into the effects
971 of alternative bed materials and additives on other phenomena driven by the alkali metal
972 content of biomass fuels, such as slagging, fouling and corrosion. Some alternatives bed
973 materials and additives have been observed to have large effects on alkali chlorides and HCl,
974 which drive corrosion within the boiler.

- 975 • There may be some interest in blending of bed materials, perhaps to balance performance
976 with cost, and investigating impact on the whole boiler system.
- 977 • There may also be some interest in trialling different dosage rates of additives from under to
978 overdosing relative to the molar amount needed for the given fuel, and investigating the
979 cost and performance impact on the whole boiler system.
- 980 • Co-firing of biomass-biomass blends and the effect on agglomeration is something that has
981 received little work outside of wood-straw mixtures. From current works, biomass ashes
982 have exhibited complex, non-linear relationships for properties such as initial ash
983 deformation temperature. Work in this area could aid in assessing the viability of such
984 blends for larger scale FBC units.
- 985 • Studies into optimising bed replenishment rates may be of interest, as no work on this area
986 seems apparent in literature. However, this may be challenging from the perspective of
987 finding a suitable and available test facility or full-scale unit on which a study could be
988 conducted.

989 **4. Agglomeration Monitoring and Prediction**

990 This section provides a brief overview and introduction to agglomeration monitoring and prediction
991 methods. A more extensive and comprehensive review of this broad field is available with the work
992 of Bartels, et al. [20].

993 These methods can fall under one of two general categories:

- 994 1. “Pre-combustion” prediction – methods applied before use of the fuel in a full scale boiler,
995 e.g. empirical correlations, lab-scale testing.
- 996 2. “In-situ” monitoring and prediction – methods that may be applied within a full-scale boiler
997 to monitor agglomeration during standard operation.

998 **4.1 Pre-combustion Prediction of Agglomeration**

999 **Experimental Methods**

1000 Several research groups have attempted to utilise standardised fuel ash testing methods to predict
1001 agglomeration temperatures. For example, the ASTM ash fusion test was performed on several
1002 biomass fuels by Skrifvars, et al. [35], though it was found to be unreliable, as it predicted
1003 problematic temperatures for ashes well in excess of the temperatures where they are known to be
1004 problematic in a fluidised bed. A sintering test was more accurate, but typically under-predicted
1005 temperatures at which ashes would be problematic by 20-50°C. At present, the most reliable
1006 experimental method for determining agglomeration difficulties associated with a new fuel may be
1007 is through lab- and pilot-scale trials.

1008 **Theoretical Methods**

1009 Use of the thermochemical software package FactSage has gained popularity in recent years as a
1010 tool to predict slagging and melting phase temperatures for fuels, as the available databases have
1011 improved in breadth and accuracy [77, 96]. The work of Fryda, et al. [97], whilst using older
1012 databases, is an example of FactSage being used to predict melt formation fractions across typical
1013 FBC operating temperatures. A point of note here is that there was a prediction of 25-45% less melt
1014 formed when the silica in bed material did not react with fuel ash elements. Fryda, et al. [97] note
1015 that this was more realistic for their fuels, as from their SEM/EDS observations there was not
1016 significant interactions between bed material and fuel ash. As Fryda, et al. [97] state, this highlights
1017 some general shortfalls of FactSage modelling, in that it considers all silica equally reactive, and does
1018 not have any allowance for bed material porosity or size, leading to the suggestion that only a

1019 fraction of silica in the bed material should be considered within the FactSage model. More
1020 generally, this reinforces the necessity of having a good understanding of the real phenomena in
1021 order to create an accurate model.

1022 The more recent work of Rizvi, et al. [96] examined slag formation quantities and compositions using
1023 FactSage, for pine wood, peanut shells, sunflower stalks, and miscanthus. All fuels were predicted to
1024 have some liquid slag formation at 700°C, however each fuel had different responses to increases in
1025 temperature. For example, both peanut ash and pine wood maintained relatively constant liquid slag
1026 fractions through typical FBC operating temperatures of 800-900°C. Miscanthus on the other hand
1027 exhibited a 10-15% increase. It should be noted though that this work does not consider the fuel in
1028 the presence of the bed material, only the fuel alone, and doing so would likely encounter many of
1029 the similar challenges highlighted by Fryda, et al. [97].

1030 **Indices**

1031 Numerous empirical agglomeration indices have been proposed over the years by researchers.
1032 Gatternig [98, p. 56] provided a summary of common agglomeration indices and relationships for
1033 both coal and biomass. The coal indices tested on biomass, as well as those proposed for biomass,
1034 have been reproduced and further added to in Table 6.

1035 These indices have varying levels of usefulness. The Alkali Index has been examined by several
1036 researchers, and provides a generally good indication of the likelihood of fouling, slagging, or
1037 agglomeration, but its effectiveness decreases when other factors are at play such as alternate bed
1038 materials and/or additives [90, 99, 100]. The alkaline earth oxides to alkaline oxides ratio examined
1039 by Fernández Llorente & Carrasco García [101] was found to provide a poor indication of the
1040 likelihood and severity of ash sintering. Therefore, it is important to consider the combustion
1041 conditions under which the fuel will be used when applying an agglomeration indicator, as these
1042 indicators have been empirically derived and may not be directly applicable.

1043 **4.2 In-situ Monitoring and Prediction of Agglomeration**

1044 **Pressure Drop**

1045 Pressure drop across the bed is a common reading taken on FBC units, with it giving operators real-
1046 time information on bed hydrodynamics and fluidisation behaviour, as well as density and height
1047 [20, 102]. However, bed pressure drop only gives a view of the bed as a singular entity, with the
1048 potential for smaller scale disturbances going unnoticed. Moreover, probe blockages may cause
1049 measurement inaccuracies.

1050 Nonetheless, researchers have tried to apply algorithms or statistical analyses to detect when
1051 agglomeration or a defluidization event may be beginning [20]. For example, Chirone, et al. [51]
1052 looked at pressure drop variance, and noted a 60% decline in pressure drop variance had occurred at
1053 the point of defluidization, with similar observations noted in a subsequent work [47].

1054 **Temperature**

1055 Temperatures are routinely measured on FBC units, often in several locations within the bed.
1056 Moreover, as has been seen in sections 2 and 3, operating temperature has a large impact on melt
1057 formation and the likelihood of other phenomena such as sintering to worsen agglomeration. An
1058 issue with this approach is successfully determining a localised spike due to agglomerate formation
1059 versus one that is the result of normal variances during combustion. Furthermore, full coverage of
1060 the bed with thermocouples is not possible, as there is always the possibility of missing small,
1061 localised variations of importance [103]. Some authors have evaluated the potential for
1062 temperature-based detection of hot-spots and agglomerate formation. For example, Khan and
1063 Turton [104] used thermocouple data and empirically derived heat transfer coefficients to analyse
1064 temperature variations within the bed, whilst Basu [105] applied a statistical analysis to highlight
1065 abnormal temperature variances within the bed. Lau & Whalley [106] trialled radially mounted
1066 differential thermocouples to detect hotspots when combusting caking coals with some success,
1067 though this was in the context of a lab-scale wall-heated FBC unit.

1068 **Other Methods**

1069 Several novel methods for agglomeration detection have been trialled over the years. One example
1070 is the use of fibre optic sensors to measure bed hydrodynamic data, though this has been restricted
1071 to lab-scale units [107, 108, 109, 110].

1072 The work of Wang, et al. [102] trialled analysis of acoustic emissions, resultant from inter-particle
1073 and particle-wall collisions. It was shown that there was potential with this methodology, given
1074 sufficient data and a competent interpretive model. Others have since expanded upon acoustic
1075 emissions monitoring methods and the associated mathematical analyses to the point where specific
1076 agglomerates can be identified, though further development is needed to improve reliability and
1077 scale them up for full-scale FBC units [111, 112, 113].

1078 **Combined Approaches**

1079 Some researchers have attempted to combine monitoring approaches to see if the result is more
1080 accurate for detecting agglomeration and defluidization. An example is the recent work of
1081 Shabanian, et al. [114] where bed pressure drop and temperatures were considered together.
1082 Shabanian, et al. [114] took reference values for the temperature difference between an upper and
1083 lower point in the bed, as well as pressure difference between an upper lower point in the bed, and
1084 then compared a moving average of real temperature and pressure differences against these
1085 reference values. From this, they were able to derive settings that could be used as “high” and “high-
1086 high” alarm points, warning of defluidization. In some cases, their method gave indication of
1087 defluidization upwards of 3 hours in advance. This highlights that there may be some considerable
1088 promise in combined approaches to agglomeration monitoring, though still leaves open the question
1089 of mitigation and prevention.

1090 **4.3 Summary of Agglomeration Monitoring and Prediction Methods**

1091 Monitoring and prediction of agglomeration is an area where much work is still needed to create
1092 accurate, robust, reliable, and cost effective solutions. Empirical indices appear to require further
1093 refining across a variety of fuels, conditions, and scales to be of more use, and to do so would likely
1094 take large collaborative efforts to collect, compile and analyse the necessary data. Lab-scale
1095 combustion trials of fuels are perhaps the best way to assess its issues prior to use at the full scale,
1096 but numerous tests may be needed to represent the range of fuel qualities that a facility may use,
1097 and this would increase the cost and time requirements of such studies. For in-situ monitoring,
1098 pressure drop and temperature based methods are preferred as such measurements are readily
1099 available on industrial units, however there are still challenges in drawing accurate and reliable
1100 correlations for the prediction of agglomeration and defluidization. Combined approaches such as
1101 that of Shabanian, et al. [114] have been shown to have some promise, and developments along
1102 similar lines may be worthwhile.

1103 **5. Conclusion**

1104 Sections 2.4, 3.13, 4.3 provide more detailed summaries and suggestions for further work for each
1105 area examined within this review. The main findings from this review are as follows:

- 1106 • There is a wealth of mechanism research when combusting biomass on SiO₂-based bed
1107 materials, with agglomeration mechanisms being of the coating- or melt-induced variety. For
1108 coating agglomeration in the case of SiO₂-based bed materials, there is the common
1109 occurrence of two or three distinct particle layers, with a higher presence of potassium
1110 within the fuel causing the “inner-inner” third layer. Sufficient growth of the calcium-based
1111 “inner” layer appears to prevent further formation of K-silicate melts with the bed particle,
1112 and as the layer changes in composition further diffusion of calcium is limited. Melt-induced
1113 agglomeration is the result of sufficient silica and alkali metal content in the fuel forming an
1114 ash melt. In some cases, the ash skeleton shape of the particle appears to allow the

1115 formation of agglomerates similar in shape to that of the fuel particle. Further work is
1116 particularly needed into mechanisms when using alternate bed materials and additives, with
1117 consideration given to the effects on the whole boiler system.

- 1118 • Of the operating variables, fuel, bed material, additives, fluidizing gas velocity and
1119 temperature have the greatest effect on agglomeration severity. An overall ranking of
1120 parameters examined is given in Table 5. Most other variables have received some degree of
1121 attention, though may benefit from some deeper studies. Co-firing of dual-biomass blends
1122 stands out as one area that may benefit from additional work, given that work so far has
1123 focused on coal-biomass or wood-straw mixes, together with further work into alternative
1124 bed materials and additives.
- 1125 • A brief overview of agglomeration monitoring and prediction methods has been given,
1126 showing that whilst there are numerous potential methods available, accuracy is a key
1127 concern. Monitoring and prediction is in general an area that would benefit from further
1128 work into accurate, reliable, robust and cost-effective monitoring and prediction methods
1129 for full-scale installations. Recent work on combined approaches using temperature and
1130 pressure drop measurements has shown some promise in this field, where defluidization
1131 was successfully predicted up to 3 hours in advance.

1132 **Acknowledgements**

1133 The authors acknowledge UK EPSRC funding support through research grant no. EP/M01536X/1 and
1134 EPSRC Centre for Doctoral Training in CCS and Cleaner Fossil Energy, grant no. EP/L016362/1.

1135 **6. References**

1136

- [1] Frankfurt School of Finance and Management, "Global Trends in Renewable Energy Investment 2016," Frankfurt School of Finance and Management, 2016.
- [2] E. Johnson, "Goodbye to carbon neutral: Getting biomass footprints right," *Environmental Impact Assessment Review*, vol. 29, no. 3, pp. 165-168, 2009.
- [3] J. Goldemberg, T. Johansson and D. Anderson, "World energy assessment: overview : 2004 update," United Nations Development Programme, New York, 2004.
- [4] Department for Business, Energy & Industrial Strategy, "Electricity Generation Costs," UK Government, 2016.
- [5] F. Johnsson, "Fluidized Bed Combustion for Clean Energy," Vancouver, Canada, 2007.
- [6] P. Basu, *Combustion and Gasification in Fluidized Beds*, 1st ed., Taylor & Francis, 2006.
- [7] J. Koornneef, M. Junginger and A. Faaij, "Development of fluidized bed combustion - An overview of trends, performance and cost," *Progress in Energy and Combustion Science*, vol. 33, pp. 19-55, 2007.
- [8] A. Hotta, "Circulating Fluidized Bed Technology," in *4th EU South Africa Clean Coal Working Group Meeting*, Kempton Park, South Africa, 2012.
- [9] A. Khan, W. de Jong, P. Jansens and H. Spliethoff, "Biomass combustion in fluidized bed boilers: Potential problems and remedies," *Fuel Processing Technology*, vol. 90, pp. 21-50, 2009.

- [10] B. Jenkins, L. Baxter, T. Miles Jr. and T. Miles, "Combustion properties of biomass," *Fuel Processing Technology*, vol. 54, pp. 17-46, 1998.
- [11] S. Vassilev, D. Baxter, L. Andersen and C. Vassileva, "An overview of the chemical composition of biomass," *Fuel*, vol. 89, no. 5, pp. 913-933, 2010.
- [12] R. Saidur, E. Abdelaziz, A. Demirbas, M. Hossain and S. Mekhilef, "A review on biomass as a fuel for boilers," *Renewable and Sustainable Energy Reviews*, vol. 15, no. 5, pp. 2262-2289, 2011.
- [13] P. Xing, P. Mason, S. Chilton, S. Lloyd, J. Jones, A. Williams, W. Nimmo and M. Pourkashanian, "A comparative assessment of biomass ash preparation methods using X-ray fluorescence and wet chemical analysis," *Fuel*, vol. 182, pp. 161-165, 2016.
- [14] M. Lackner, F. Winter and A. Agarwal, *Handbook of Combustion Vol. 4*, John Wiley & Sons, 2010.
- [15] D. Kunii and O. Levenspiel, *Fluidization Engineering*, 2nd Edition, Butterworth-Heinemann, 1991.
- [16] R. Brown, M. Dawson and J. Smeenk, "Bed Material Agglomeration During Fluidized Bed Combustion," U.S. Department of Energy, Pittsburgh, PA, 1996.
- [17] E. Zabetta, V. Barišić, K. Peltola and A. Hotta, "Foster Wheeler Experience with biomass and waste in CFBs," in *33rd International Technical Conference on Coal Utilization and Fuel Systems*, Clearwater, Florida, 2008.
- [18] A. Giramonti, R. Lessard, D. Merrick and M. Hobson, "Technical and Economic Assessment of Fluidized Bed Augmented Compressed Air Energy Storage System," Battelle Memorial Institute, 1991.

- [19] N. Kumar, P. Besuner, S. Lefton, D. Agan and D. Hilleman, "Power plant cycling costs," National Renewable Energy Laboratory, Sunnyvale, California, 2012.
- [20] M. Bartels, W. Lin, J. Nijenhuis, F. Kapteijn and J. van Ommen, "Agglomeration in fluidized beds at high temperatures: Mechanisms, detection and prevention," *Progress in Energy and Combustion Science*, vol. 34, no. 5, pp. 633-666, 2008.
- [21] P. Basu, C. Kefa and L. Jestin, *Boilers and Burners: Design and Theory*, Springer, 2000.
- [22] Y. Niu, Y. Zhu, H. Tan, S. Hui, Z. Jing and W. Xu, "Investigations on biomass slagging in utility boiler: Criterion numbers and slagging growth mechanisms," *Fuel Processing Technology*, vol. 128, pp. 499-508, 2014.
- [23] A. Stam, K. Haasnoot and G. Brem, "Superheater fouling in a BFB boiler firing wood-based fuel blends," *Fuel*, vol. 135, pp. 322-331, 2014.
- [24] H. Nielsen, F. Frandsen, K. Dam-Johansen and L. Baxter, "The implications of chlorine-associated corrosion on the operation of biomass-fired boilers," *Progress in energy and combustion science*, vol. 26, no. 3, p. 283-298, 2000.
- [25] P. Henderson, P. Szakálos, R. Pettersson, C. Andersson and J. Högberg, "Reducing superheater corrosion in wood-fired boilers," *Materials and Corrosion*, vol. 57, no. 2, pp. 128-134, 2006.
- [26] H. Kassman, M. Broström, M. Berg and L. Åmand, "Measures to reduce chlorine in deposits: Application in a large-scale circulating fluidised bed boiler firing biomass," *Fuel*, vol. 60, no. 4, pp. 1325-1334, 2011.
- [27] A. Demirbas, "Potential applications of renewable energy sources, biomass combustion problems in boiler power systems and combustion related environmental issues," *Progress in Energy and Combustion Science*, vol. 31, no. 2, pp. 171-192, 2005.

- [28] G. Olofsson, Z. Ye, I. Bjerle and A. Andersson, "Bed Agglomeration Problems in Fluidized-Bed Biomass Combustion," *Industrial & Engineering Chemistry Research*, vol. 41, no. 12, pp. 2888-2894, 2002.
- [29] M. Radovanovic, *Fluidized Bed Combustion*, Taylor & Francis, 1986.
- [30] A. Ghaly, A. Ergüdenler and E. Laufer, "Agglomeration characteristics of alumina sand-straw ash mixtures at elevated temperatures," *Biomass and bioenergy*, vol. 5, no. 6, p. 467-480, 1993.
- [31] A. Ghaly, A. Ergüdenler and E. Laufer, "Study of agglomeration characteristics of silica sand-straw ash mixtures using scanning electronic microscopy and energy dispersion X-ray techniques," *Bioresource technology*, vol. 48, no. 2, p. 127-134, 1994.
- [32] A. Nordin, M. Öhman, B. Skrifvars and M. Hupa, *Applications of Advanced Technology to Ash-Related Problems in Boilers*, Springer International Publishing, 1996.
- [33] B. Skrifvars, M. Hupa, R. Backman and M. Hiltunen, "Sintering mechanisms of FBC ashes," *Fuel*, vol. 73, no. 2, pp. 171-176, 1994.
- [34] B. Skrifvars, R. Backman and M. Hupa, "Characterization of the sintering tendency of ten biomass ashes in FBC conditions by a laboratory test and by phase equilibrium calculations," *Fuel Processing Technology*, vol. 56, no. 1, pp. 55-67, 1998.
- [35] B. Skrifvars, M. Öhman, A. Nordin and M. Hupa, "Predicting bed agglomeration tendencies for biomass fuels fired in FBC boilers: a comparison of three different prediction methods," *Energy & Fuels*, vol. 13, no. 2, pp. 359-363, 1999.
- [36] M. Öhman and A. Nordin, "Bed Agglomeration Characteristics during Fluidized Bed Combustion of Biomass Fuels," *Energy & Fuels*, vol. 14, pp. 169-178, 2000.

- [37] M. Öhman and A. Nordin, "A new method for quantification of fluidized bed agglomeration tendencies: a sensitivity analysis," *Energy & Fuels*, vol. 12, no. 1, p. 90–94, 1998.
- [38] J. Silvennoinen, "A new method to inhibit bed agglomeration problems in fluidized bed boilers," Jacksonville, Florida, 2003.
- [39] L. Nuutinen, M. Tiainen, M. Virtanen, S. Enestam and R. Laitinen, "Coating Layers on Bed Particles during Biomass Fuel Combustion in Fluidized-Bed Boilers," *Energy & Fuels*, vol. 18, no. 1, pp. 127-139, 2004.
- [40] H. Visser, "The Influence of Fuel Composition on Agglomeration Behaviour in Fluidised-Bed Combustion," Energy Research Centre of the Netherlands (ECN), 2004.
- [41] E. Brus, M. Öhman and A. Nordin, "Mechanisms of Bed Agglomeration during Fluidized-Bed Combustion of Biomass Fuels," *Energy & Fuels*, vol. 19, no. 3, pp. 825-832, 2005.
- [42] M. Öhman, L. Pommer and A. Nordin, "Bed Agglomeration Characteristics and Mechanisms during Gasification and Combustion of Biomass Fuels," *Energy & Fuels*, vol. 19, no. 4, pp. 1742-1748, 2005.
- [43] M. Zevenhoven-Onderwater, M. Öhman, B. Skrifvars, R. Backman, A. Nordin and M. Hupa, "Bed Agglomeration Characteristics of Wood-Derived Fuels in FBC," *Energy & Fuels*, vol. 20, no. 2, pp. 818-824, 2006.
- [44] A. Grimm, M. Öhman, T. Lindberg, A. Fredriksson and D. Boström, "Bed Agglomeration Characteristics in Fluidized-Bed Combustion of Biomass Fuels Using Olivine as Bed Material," *Energy & Fuels*, vol. 26, no. 7, pp. 4550-4559, 2012.

- [45] H. He, D. Boström and M. Öhman, "Time Dependence of Bed Particle Layer Formation in Fluidized Quartz Bed Combustion of Wood-Derived Fuels," *Energy & Fuels*, vol. 28, no. 6, pp. 3841-3848, 2014.
- [46] B. Gatternig and J. Karl, "Investigations on the Mechanisms of Ash-Induced Agglomeration in Fluidized-Bed Combustion of Biomass," *Energy & Fuels*, vol. 29, pp. 931-941, 2015.
- [47] F. Scala and R. Chirone, "Characterization and Early Detection of Bed Agglomeration during the Fluidized Bed Combustion of Olive Husk," *Energy & Fuels*, vol. 20, no. 1, pp. 120-132, 2006.
- [48] H. He, X. Ji, D. Boström, R. Backman and M. Öhman, "Mechanism of Quartz Bed Particle Layer Formation in Fluidized Bed Combustion of Wood Derived Fuels," *Energy & Fuels*, vol. 30, no. 3, pp. 2227-2232, 2016.
- [49] B. Gatternig and J. Karl, "The Influence of Particle Size, Fluidization Velocity, and Fuel Type on Ash-Induced Agglomeration in Biomass Combustion," *Frontiers in Energy Research*, vol. 2, 2014.
- [50] W. Lin, K. Dam-Johansen and F. Frandsen, "Agglomeration in bio-fuel fired fluidized bed combustors," *Chemical Engineering Journal*, vol. 96, pp. 171-185, 2003.
- [51] R. Chirone, F. Miccio and F. Scala, "Mechanism and prediction of bed agglomeration during fluidized bed combustion of a biomass fuel: Effect of the reactor scale," *Chemical Engineering Journal*, vol. 123, no. 3, pp. 71-80, 2006.
- [52] H. Liu, Y. Feng, S. Wu and D. Liu, "The role of ash particles in the bed agglomeration during the fluidized bed combustion of rice straw," *Bioresource Technology*, vol. 100, no. 24, pp. 6505-6513, 2009.

- [53] C. Lin and M. Wey, "The effect of mineral compositions of waste and operating conditions on particle agglomeration/defluidization during incineration," *Fuel*, vol. 83, no. 17-18, pp. 2335-2343, 2004.
- [54] W. Pietsch, *Agglomeration in Industry: Occurrence and Applications*, Wiley-VCH, 2004.
- [55] W. Pietsch, *Agglomeration Processes*, Wiley-VCH, 2008.
- [56] E. Anthony, A. Iribarne and J. Iribarne, "A new mechanism for FBC agglomeration and fouling in 100 percent firing of petroleum coke," *Journal of Energy Resources Technology*, vol. 119, no. 1, pp. 55-61, 1997.
- [57] E. Anthony, F. Preto, L. Jia and J. Iribarne, "Agglomeration and fouling in petroleum coke-fired FBC boilers," *Journal of Energy Resources Technology*, vol. 120, no. 4, pp. 285-292, 1998.
- [58] B. Skrifvars, M. Hupa and E. Anthony, "Mechanisms of bed material agglomeration in a petroleum coke-fired circulating fluidized bed boiler," *Journal of Energy Resources Technology*, vol. 120, no. 3, pp. 215-218, 1998.
- [59] R. Chirone, P. Salatino, F. Scala, R. Solimene and M. Urciuolo, "Fluidized bed combustion of pelletized biomass and waste-derived fuels," *Combustion and Flame*, vol. 155, no. 1-2, pp. 21-36, 2008.
- [60] F. Scala and R. Chirone, "An SEM/EDX study of bed agglomerates formed during fluidized bed combustion of three biomass fuels," *Biomass and Bioenergy*, vol. 32, no. 3, pp. 252-266, 2008.
- [61] C. Yu, J. Qin, H. Nie, M. Fang and Z. Luo, "Experimental research on agglomeration in straw-fired fluidized beds," *Applied Energy*, vol. 88, no. 12, pp. 4534-4543, 2011.

- [62] C. Zhou, C. Rosen and K. Engvall, "Biomass oxygen/steam gasification in a pressurized bubbling fluidized bed: Agglomeration behavior," *Applied Energy*, vol. 172, pp. 230-250, 2016.
- [63] J. Grace, "Contacting modes and behaviour classification of gas—solid and other two-phase suspensions," *The Canadian Journal of Chemical Engineering*, vol. 64, no. 3, p. 353–363, 1986.
- [64] P. Chaivatamaset, P. Sricharoon and S. Tia, "Bed agglomeration characteristics of palm shell and corncob combustion in fluidized bed," *Applied Thermal Engineering*, vol. 31, no. 14-15, pp. 2916-2927, 2011.
- [65] C. Lin, T. Peng and W. Wang, "Effect of particle size distribution on agglomeration/defluidization during fluidized bed combustion," *Powder Technology*, vol. 207, no. 1-3, pp. 290-295, 2011.
- [66] J. Howard, *Fluidized Bed Technology: Principles and Applications*, Adam Hilger Ltd., 1989.
- [67] S. Oka, *Fluidized Bed Combustion*, CRC Press, 2003.
- [68] J. Kuo, W. Hsu and T. Yo, "Effect of air distribution on solid fuel bed combustion," *Transactions - American Society of Chemical Engineers Journal of Energy Resources Technology*, vol. 119, pp. 120-128, 1997.
- [69] S. Chilton, *The Combustion of Low Grade Fuels in Fluidised Bed Combustors*, University of Leeds, 2017.
- [70] R. Darton, "Bubble growth due to coalescence in fluidised beds," *Transactions of the Institute of Chemical Engineers*, vol. 55, pp. 274-280, 1977.
- [71] M. Hupa, "Interaction of fuels in co-firing in FBC," *Fuel*, vol. 80, no. 10, pp. 1312-1319, 2005.

- [72] K. Davidsson, L. Åmand, B. Steenari, A. Elled, D. Eskilsson and B. Leckner, "Countermeasures against alkali-related problems during combustion of biomass in a circulating fluidized bed boiler," *Chemical Engineering Science*, vol. 63, no. 21, pp. 5314-5329, 2008.
- [73] M. Hupa, O. Karlström and E. Vainio, "Biomass combustion technology development – It is all about chemical details," *Proceedings of the Combustion Institute*, vol. 36, no. 1, pp. 113-134, 2017.
- [74] D. Salour, B. Jenkins, M. Vafaei and M. Kayhanian, "Control of in-bed agglomeration by fuel blending in a pilot scale straw and wood fueled AFBC," *Biomass and Bioenergy*, vol. 4, no. 2, pp. 117-133, 1993.
- [75] K. Davidsson, L. Åmand, A. Elled and B. Leckner, "Effect of Cofiring Coal and Biofuel with Sewage Sludge on Alkali Problems in a Circulating Fluidized Bed Boiler," *Energy & Fuels*, vol. 21, no. 6, pp. 3180-3188, 2007.
- [76] P. Thy, B. Jenkins, R. Williams, C. Leshner and R. Bakker, "Bed agglomeration in fluidized combustor fueled by wood and rice straw blends," *Fuel Processing Technology*, vol. 91, no. 11, pp. 1464-1485, 2010.
- [77] A. Elled, L. Åmand and B. Steenari, "Composition of agglomerates in fluidized bed reactors for thermochemical conversion of biomass and waste fuels," *Fuel*, vol. 111, pp. 696-708, 2013.
- [78] J. Silvennoinen and M. Hedman, "Co-firing of agricultural fuels in a full-scale fluidized bed boiler," *Fuel Processing Technology*, vol. 105, pp. 11-19, 2013.
- [79] M. Becidan, E. Houshfar, R. Khalil, Ø. Skreiberg, T. Løvås and L. Sørum, "Optimal Mixtures to Reduce the Formation of Corrosive Compounds during Straw Combustion: A Thermodynamic Analysis," *Energy & Fuels*, vol. 25, no. 7, pp. 3223-3234, 2011.

- [80] P. Suheri and V. Kuprianov, "Co-Firing of Oil Palm Empty Fruit Bunch and Kernel Shell in a Fluidized-Bed Combustor: Optimization of Operating Variables," *Energy Procedia*, vol. 79, pp. 956-962, 2015.
- [81] K. Sirisomboon and V. Kuprianov, "Effects of Fuel Staging on the NO Emission Reduction during Biomass–Biomass Co-combustion in a Fluidized-Bed Combustor," *Energy & Fuels*, vol. 31, no. 1, pp. 659-671, 2017.
- [82] A. Burton and H. Wu, "Influence of biomass particle size on bed agglomeration during biomass pyrolysis in fluidised bed," *Proceedings of the Combustion Institute*, vol. 36, no. 2, pp. 2199-2205, 2017.
- [83] H. Li, Q. Chen, X. Zhang, K. Finney, V. Sharifi and J. Swithenbank, "Evaluation of a biomass drying process using waste heat from process industries: A case study," *Applied Thermal Engineering*, vol. 35, pp. 71-80, 2012.
- [84] P. Knutsson, G. Schwebel, B. Steenari and H. Leion, "Effect of bed materials mixing on the observed bed sintering," Beijing, China, 2014.
- [85] A. Corcoran, J. Marinkovic, F. Lind, H. Thunman, P. Knutsson and M. Seemann, "Ash Properties of Ilmenite Used as Bed Material for Combustion of Biomass in a Circulating Fluidized Bed Boiler," *Energy & Fuels*, vol. 28, pp. 7672-7679, 2014.
- [86] L. Bierlein and B. Fredriksson-Moeller, "New Industrial Development in Fluidised Bed Combustion of Waste and Biomass," in *25th European Biomass Conference and Exhibition*, Stockholm, Sweden, 2017.
- [87] D. Geldart, "Types of Gas Fluidization," *Powder Technology*, vol. 7, pp. 285-292, 1973.

- [88] B. Steenari and O. Lindqvist, "High-temperature reactions of straw ash and the anti-sintering additives kaolin and dolomite," *Biomass and Bioenergy*, vol. 14, no. 1, p. 67–76, 1998.
- [89] M. Öhman and A. Nordin, "The Role of Kaolin in Prevention of Bed Agglomeration during Fluidized Bed Combustion of Biomass Fuels," *Energy & Fuels*, vol. 14, no. 3, pp. 618-624, 2000.
- [90] D. Vamvuka, D. Zografos and G. Alevizos, "Control methods for mitigating biomass ash-related problems in fluidized beds," *Bioresource Technology*, vol. 99, no. 9, pp. 3534-3544, 2008.
- [91] C. Lin, J. Kuo, M. Wey, S. Chang and K. Wang, "Inhibition and promotion: The effect of earth alkali metals and operating temperature on particle agglomeration/defluidization during incineration in fluidized bed," *Powder Technology*, vol. 189, no. 1, pp. 57-63, 2009.
- [92] B. Coda, M. Aho, R. Berger and K. Kein, "Behavior of chlorine and enrichment of risky elements in bubbling fluidized bed combustion of biomass and waste assisted by additives," *Energy & Fuels*, vol. 15, no. 3, p. 680–690, 2001.
- [93] J. Seville and R. Clift, "The Effect of Thin Liquid Layers on Fluidisation Characteristics," *Powder Technology*, vol. 37, pp. 117-129, 1984.
- [94] E. Brus, M. Öhman, A. Nordin, B. Skrifvars and R. Backman, "Bed Material Consumption in Biomass Fired Fluidised Bed Boilers Due to Risk of Bed Agglomeration - Coating Formation and Possibilities for Regeneration," *IFRF Combustion Journal*, 2003.
- [95] H. Visser, S. van Lith and J. Kiel, "Biomass Ash-Bed Material Interactions Leading to Agglomeration in FBC," *Journal of Energy Resources Technology*, vol. 130, no. 1, p. 011801, 2008.

- [96] T. Rizvi, P. Xing, M. Pourkashanian, L. Darvell, J. Jones and W. Nimmo, "Prediction of biomass ash fusion behaviour by the use of detailed characterisation methods coupled with thermodynamic analysis," *Fuel*, vol. 141, pp. 275-284, 2015.
- [97] L. Fryda, K. Panopoulos and E. Kakaras, "Agglomeration in fluidised bed gasification of biomass," *Powder Technology*, vol. 181, no. 3, pp. 307-320, 2008.
- [98] B. Gattermig, *Predicting Agglomeration in Biomass Fired Fluidized Beds*, Nuremberg: Friedrich-Alexander-Universität Erlangen-Nürnberg, 2015.
- [99] T. Miles, L. Baxter, R. Bryers, B. Jenkins and L. Oden, "Boiler deposits from firing biomass fuels," *Biomass and Bioenergy*, vol. 10, no. 2-3, pp. 125-138, 1996.
- [100] D. Dayton, B. Jenkins, S. Turn, R. Bakker, R. Williams, D. Belle-Oudry and L. Hill, "Release of Inorganic Constituents from Leached Biomass during Thermal Conversion," *Energy & Fuels*, vol. 13, no. 4, pp. 860-870, 1999.
- [101] M. Fernández Llorente and J. Carrasco García, "Comparing methods for predicting the sintering of biomass ash in combustion," *Fuel*, vol. 84, no. 14-15, pp. 1893-1900, 2005.
- [102] J. Wang, Y. Cao, X. Jiang and Y. Yang, "Agglomeration Detection by Acoustic Emission (AE) Sensors in Fluidized Beds," *Industrial & Engineering Chemistry Research*, vol. 48, no. 7, pp. 3466-3473, 2009.
- [103] J. Werther, "Measurement techniques in fluidized beds," *Powder Technology*, vol. 102, no. 1, pp. 15-36, 1999.
- [104] T. Khan and R. Turton, "The measurement of instantaneous heat transfer coefficients around the circumference of a tube immersed in a high temperature fluidized bed.," *International Journal of Heat and Mass Transfer*, vol. 35, no. 12, pp. 3397-3406, 1992.

- [105] P. Basu, "Heat transfer in high temperature fast fluidized beds," *Chemical Engineering Science*, vol. 45, no. 10, pp. 3123-3136, 1990.
- [106] I. Lau and B. Whalley, "A differential thermal probe for anticipation of defluidization of caking coals," *Fuel Processing Technology*, vol. 4, no. 2-3, pp. 101-115, 1981.
- [107] M. Ishida and H. Tanaka, "An optical probe to detect both bubbles and suspended particles in a three-phase fluidized bed," *Journal of Chemical Engineering of Japan*, vol. 15, no. 5, pp. 389-391, 1982.
- [108] J.-M. Schweitzer, J. Bayle and T. Gauthier, "Local gas hold-up measurements in fluidized bed and slurry bubble column," *Chemical Engineering Science*, vol. 56, pp. 1103-1110, 2001.
- [109] J. Link, C. Zeilstra, N. Deen and H. Kuipers, "Validation of a Discrete Particle Model in a 2D Spout-Fluid Bed Using Non-Intrusive Optical Measuring Techniques," *The Canadian Journal of Chemical Engineering*, vol. 82, no. 1, pp. 30-36, 2004.
- [110] S. Razzak, S. Barghi, J.-X. Zhu and Y. Mi, "Phase holdup measurement in a gas-liquid-solid circulating fluidized bed (GLSCFB) riser using electrical resistance tomography and optical fibre probe," *Chemical Engineering Journal*, vol. 147, no. 2-3, pp. 210-218, 2009.
- [111] Y. Jiang, C. Ren, Z. Huang, J. Wang, B. Jiang, J. Yang and Y. Yang, "Acoustic Emission Detection of Particle Movement in a Cross-Flow Moving Bed," *Industrial & Engineering Chemistry Research*, vol. 53, no. 10, pp. 4075-4083, 2014.
- [112] T. Sheahan and L. Briens, "Passive acoustic emission monitoring of pellet coat thickness in a fluidized bed," *Powder Technology*, vol. 286, pp. 172-180, 2015.

- [113] L. Weiguo, W. Xiaodong, W. Fenwei and W. Haiyan, "Feature extraction and early warning of agglomeration in fluidized bed reactors based on an acoustic approach," *Powder Technology*, vol. 279, pp. 185-195, 2017.
- [114] J. Shabaniyan, P. Sauriol and J. Chaouki, "A simple and robust approach for early detection of defluidization," *Chemical Engineering Journal*, vol. 313, pp. 144-156, 2017.
- [115] W. Hosford, *Materials Science: An Intermediate Text*, Cambridge University Press, 2006.
- [116] M. Fernández Llorente, R. Escalada Cuadrado, J. Murillo Laplaza and J. Carrasco García, "Combustion in bubbling fluidised bed with bed material of limestone to reduce the biomass ash agglomeration and sintering," *Fuel*, vol. 85, no. 14-15, pp. 2081-2092, 2006.
- [117] S. De Geyter, M. Öhman, D. Boström, M. Eriksson and A. Nordin, "Effects of Non-Quartz Minerals in Natural Bed Sand on Agglomeration Characteristics during Fluidized Bed Combustion of Biomass Fuels," *Energy & Fuels*, vol. 21, no. 5, pp. 2663-2668, 2007.
- [118] R. Liu, B. Jin, Z. Zhong and J. Zhao, "Reduction of Bed Agglomeration in CFB Combustion Biomass with Aluminium-Contain Bed Material," *Process Safety and Environmental Protection*, vol. 85, no. 5, pp. 441-445, 2007.
- [119] D. Vamvuka and D. Zografos, "Predicting the behaviour of ash from agricultural wastes during combustion," *Fuel*, vol. 83, no. 14-15, pp. 2051-2057, 2004.

1137

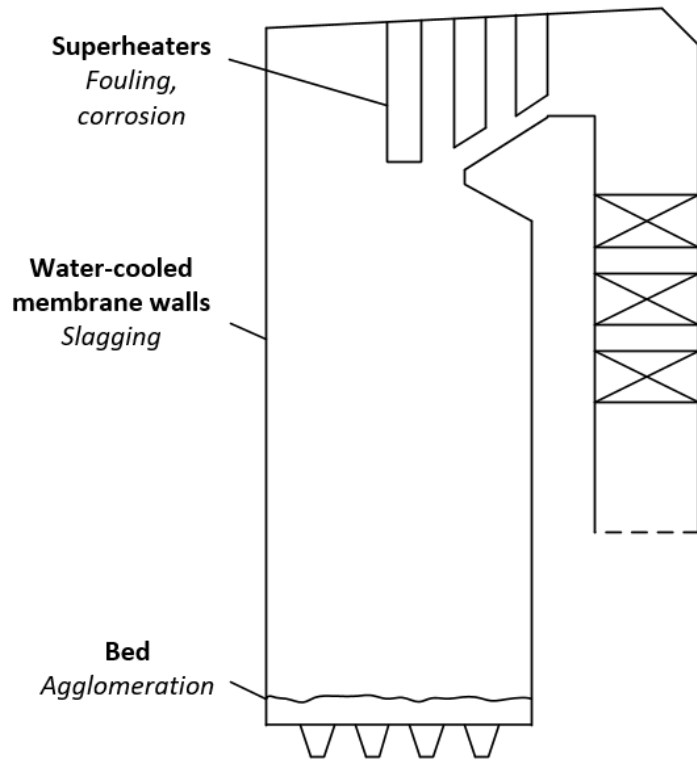
1138

1139 **7. Figures**



1140

1141 **Figure 1: Image of several agglomerate samples collected from 50kW_{th} Fluidized Bed combusting**
1142 **wheat straw pellets.**



1143

1144 **Figure 2: Simplified diagram of a BFB boiler highlighting areas where biomass ash contents - alkali**
 1145 **and alkali earth metal, silica and chlorine - cause issues. Adapted from the diagram of Hupa, et al.**
 1146 **[73].**

Three-layer coating: K-rich system

Two-layer coating: K-lean system



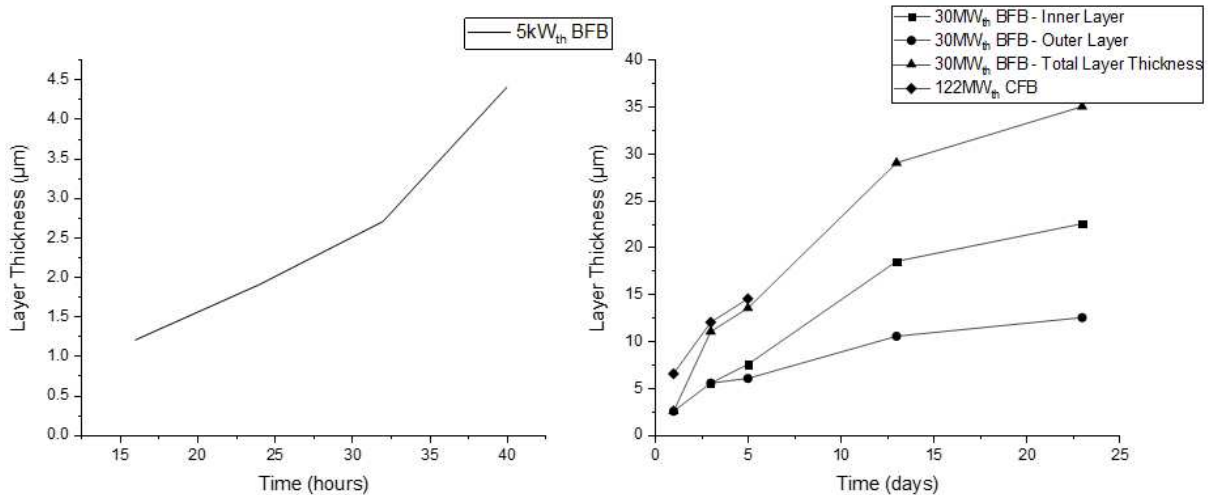
	Outer Layer	Inner Layer	Inner-Inner Layer
Element	wt%	wt%	wt%
Si	3	14-18	34
P	6	-	-
S	4	-	-
K	7	-	10
Ca	29	44	4-5

	Outer Layer	Inner Layer
Element	wt%	wt%
Si	3	14
P	5	-
S	4	-
K	7	-
Ca	28	41

1148

1149 **Figure 3: Diagram showing the compositional differences between two- and three-layer coating**

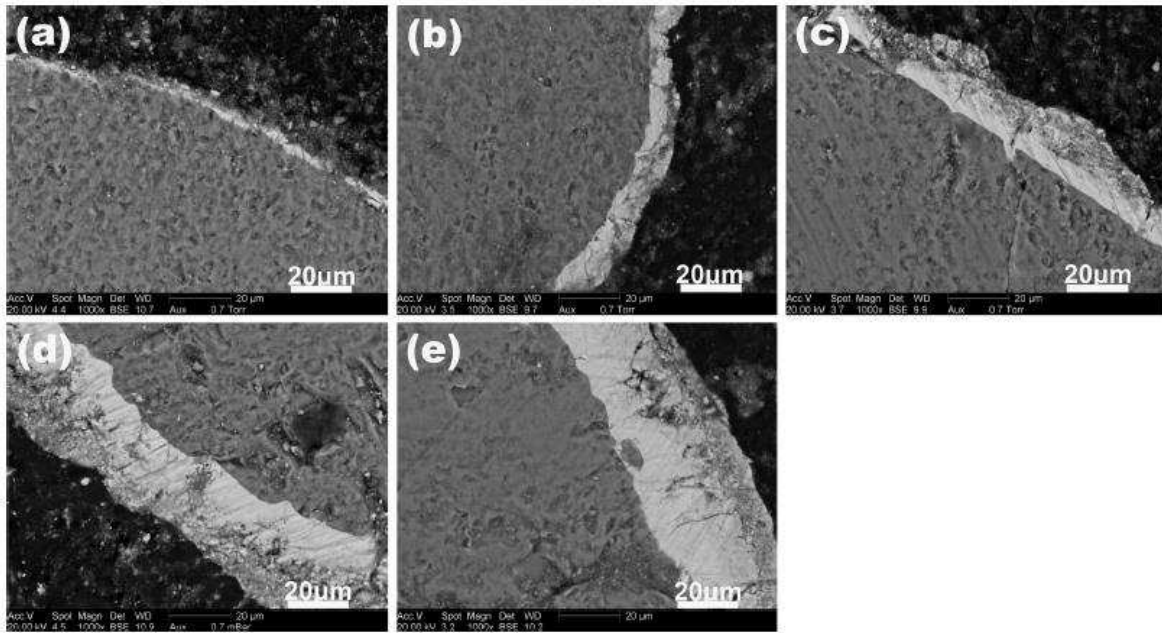
1150 **systems, as described by Visser [40]. Based on the diagram of Visser [40].**



1151

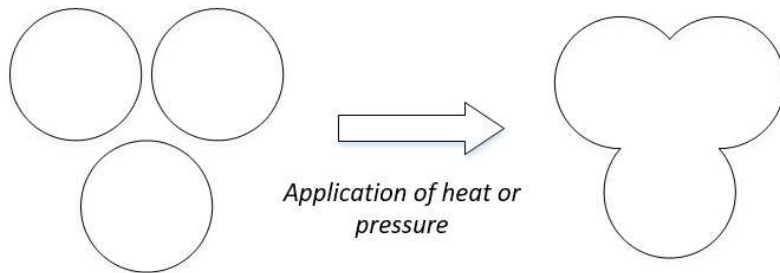
1152 **Figure 4: Coating layer growth over time for lab-scale BFB and full-scale BFB and CFB units. Based**

1153 **on the data of He, et al. [45].**



1154

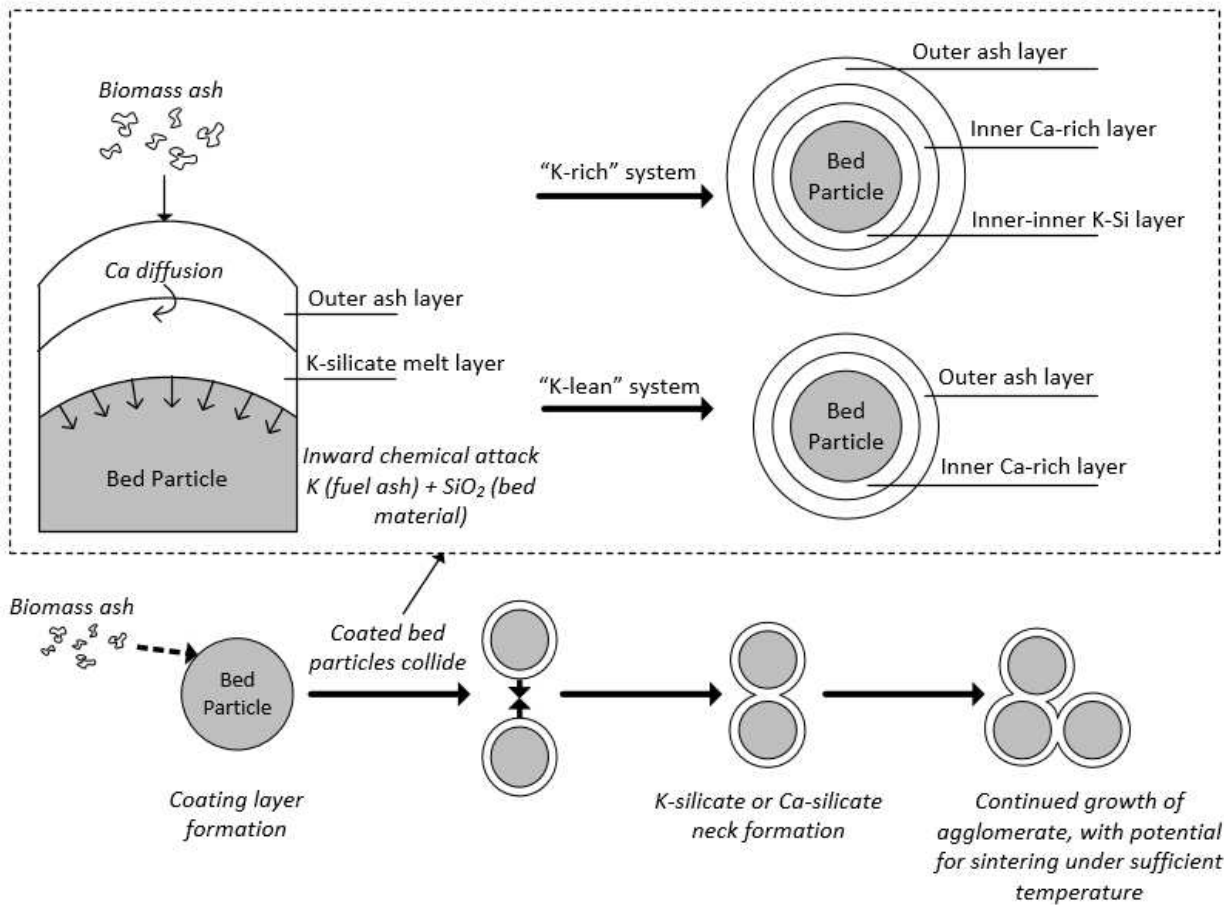
1155 **Figure 5: Example SEM images of coating layers (lighter grey) resulting from the combustion of**
 1156 **wood on a sand bed in a 30MW_{th} Bubbling FBC unit. Images ‘a’ through ‘e’ are of particles 1, 3, 5,**
 1157 **13, and 23 days after initial bed start-up. Differences in layer homogeneity moving outward can be**
 1158 **clearly seen in images ‘c’ through ‘e’. Images reproduced with permission from the work of He, et**
 1159 **al. [45].**



1160

1161 **Figure 6: Generalised diagram showing the progression of sintering. Within an atmospheric**
 1162 **fluidised bed, particles may be fused together under high temperatures. Diagram adapted from**
 1163 **Hosford [115, p. 144].**

Coating-induced Agglomeration Mechanism - SiO_2 -based Bed Material



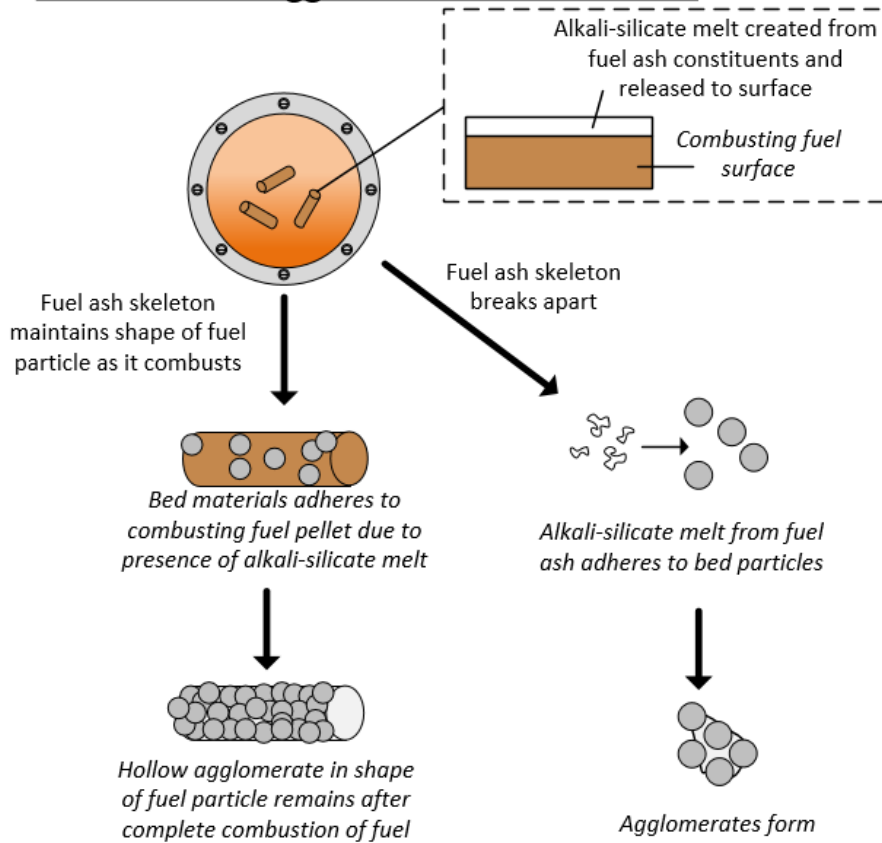
1164

1165 **Figure 7: Coating-induced agglomeration mechanism in a system with an SiO_2 -based bed material,**

1166 **whereby agglomeration proceeds due to potassium presence within the fuel ash. Described within**

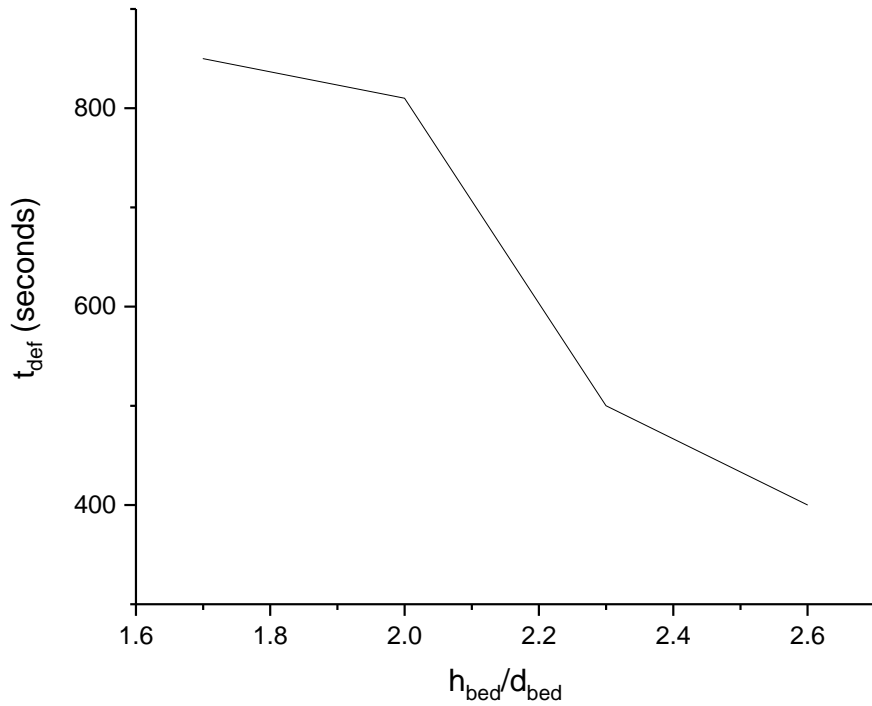
1167 **the text of section 2.4.**

Melt-induced Agglomeration Mechanism



1168

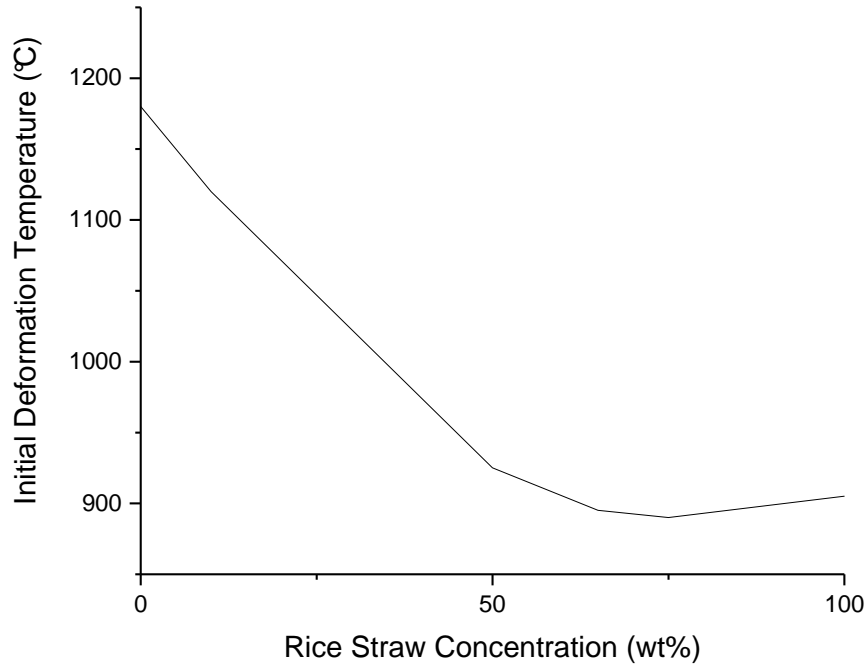
1169 **Figure 8: Melt-induced agglomeration mechanism, as described within the text of section 2.4.**



1170

1171 **Figure 9: Graph showing the effect of changing the bed height-to-diameter ratio, h_{bed}/d_{bed} , on the**

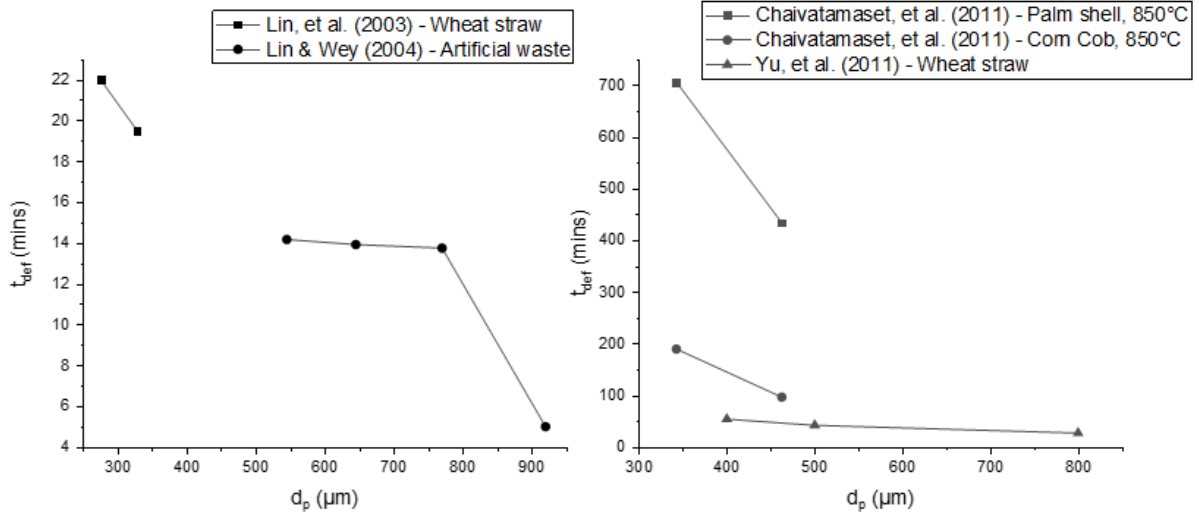
1172 **defluidization time, t_{def} . Based on the work of Lin & Wey [53].**



1173

1174 **Figure 10: Variations in initial deformation temperature (IDT) for Rice Straw/Wood fuel blend.**

1175 **Reproduced from the work of Salour, et al. [74].**



1176

1177 **Figure 11: Graphs showing the effect of changing average bed particle size on defluidization time,**
 1178 **t_{def} . Based on the works of Lin, et al. [50], Lin & Wey [53], Chaivatamaset, et al. [64], and Yu, et al.**
 1179 **[61].**

1180

1181 **8. Tables**

1182 **Table 1: Table summarising fuel and relative presence of coating on the particles examined with**
 1183 **SEM/EDS [42]. Note that this percentage presence of coating was found to be identical for both**
 1184 **combustion and gasification environments.**

Fuel	Amount of particles examined where coating was present
Bark	“Majority”
Reed canary grass	10%
Lucerne	10%
Olive flesh	“Majority”
Cane trash	10-30%
Bagasse	<10%

1185

1186 **Table 2: Coating-induced agglomeration layer growth mechanisms proposed by He, et al. [48].**

1187 **Table reproduced from He, et al. [48].**

Phase	Controlled Process	Main Crystalline Phases	Layer Growth Rate
1 (<1 day)	Reaction	Only K-rich silicate melt	Fast in the presence of enough available calcium
2 (from 1 day to ~2 weeks)	Diffusion	CaSiO ₃ , Ca ₂ SiO ₄	Medium
3 (from ~>2 weeks)	Diffusion	Ca ₂ SiO ₄ , Ca ₃ SiO ₅	Quite low

1188

1189

1190 **Table 3: Table summarising the effect of varying bed material on agglomeration. Results taken from the literature as noted.**

Reference	Bed Material	Composition	Fuel(s)	Effect on Agglomeration
Olofsson, et al. [28]	Bone ash	44.2wt% CaO, 28.8wt% P ₂ O ₃	Straw	Reduced agglomeration tendency compared to quartz sand
Olofsson, et al. [28]	Mullite	75.2wt% Al ₂ O ₃ , 24.5wt% SiO ₂	Straw	Reduced agglomeration tendency compared to quartz sand and better than Bone ash or Magnesite. Noted as being due to high melting point of alumina silicates.
Olofsson, et al. [28]	Magnesite	84.4wt% MgO, 7.55wt% CaO, 3.93wt% SiO ₂	Straw	Reduced agglomeration tendency compared to quartz sand
Nuutinen, et al. [39]	GR Granule (commercial/proprietary)	Proprietary (Mg-based, SiO ₂ -free)	Various: woody, wastes, industrial residues	Prevented agglomeration in cases where quartz sand otherwise did
Fernández Llorente, et al. [116]	Limestone	CaCO ₃	Brassica, Thistle, Almond shells	Prevented agglomeration in cases where quartz sand otherwise did
De Geyter, et al. [117]	Potassium feldspar	66.2wt% SiO ₂ , 19.3wt% Al ₂ O ₃ , 8.2wt% K ₂ O	Bark, olive residue, wheat straw	Increased agglomeration risk with bark and olive residues, no effect on wheat straw (agglomeration still occurred). Note that K-feldspar may be a constituent of natural sand.
De Geyter, et al. [117]	Plagioclase	54wt% SiO ₂ , 27wt% Al ₂ O ₃ , 11wt% CaO	Bark, olive residue, wheat straw	Increased T _{aggl} for olive residue, no effect on bark, no effect on wheat straw (agglomeration still occurred). Note that Plagioclase may be a constituent of natural sand.
De Geyter, et al. [117]	Olivine	49.5wt% MgO 45.0wt% SiO ₂	Bark, olive residue, wheat straw	Increased t _{def} for olive residue, no effect with bark, no effect on wheat straw (agglomeration still occurred)

Reference	Bed Material	Composition	Fuel(s)	Effect on Agglomeration
Liu, et al. [118]	Aluminous bed material	75.93wt% Al ₂ O ₃ , 19.92wt% SiO ₂	Cotton stalk	Agglomeration issues after 38h of operation, as opposed to 8h for silica sand, when using 200kW _{th} CFB.
Davidsson, et al. [75]	Olivine	(Mg, Fe) ₂ SiO ₄	80% woody + 20% straw blend (energy basis)	Higher T _{aggl} compared to sand. No reaction between melt-layers and Olivine. Agglomerates formed over time due to presence of straw & melt-induced agglomeration.
Davidsson, et al. [75]	Blast furnace slag	Ca/Mg/Al silicates	80% woody + 20% straw blend (energy basis)	Higher T _{aggl} compared to sand and Olivine. No reaction between melt-layers and blast furnace slag. Agglomerates formed over time due to presence of straw leading to melt-induced agglomeration.
Yu, et al. [61]	Aluminous bed material	Al ₂ O ₃	Rice straw	Increase in t _{def} though melt-induced agglomeration still occurred due to fuel.
Corcoran, et al. [85]	Quartz sand + Ilmenite (up to 40wt%)	FeTiO ₃	Wood chips	Reduction in agglomeration tendency – potassium diffused into the centre of the bed particle thus was less available to form alkali-silicate melts.
Grimm, et al. [44]	Olivine	49.0wt% MgO, 41.0wt% SiO ₂ , 8.4wt% Fe ₂ O ₃	Willow, wood residues, wheat straw, wheat distiller's dried grain with solubles (DDGS)	Fewer agglomerates with willow & wood residues compared to quartz sand bed, plus different coating layer composition (Mg/Si/Ca vs. Si/K/Ca). No reduction in agglomeration tendency with wheat straw or DDGS.

1192 **Table 4: Summary of the effects Bed Particle Diameter variations from the work of Scala & Chirone**
1193 **[60], using a quartz sand bed.**

Fuel	Temperature (°C)	Fluidizing Gas Velocity (m/s)	Excess Air (%)	d_p (μm)	t_{def} (mins)
Virgin Olive Husk	850	0.61	77	212-400	197
Virgin Olive Husk	850	0.61	76	600-850	348
Pine Seed Shells	850	0.55	35	212-400	320
Pine Seed Shells	850	0.50	75	212-400	388
Pine Seed Shells	850	0.54	58	600-850	702

1194

1195

1196 **Table 5: Table summarising the effect of various operational variables on reducing agglomeration severity.**

Effect on REDUCING Agglomeration Severity			
Conflicting or Unknown	No Effect	Minor	Major
Increase/Decrease Bed Height	Increase/Decrease Pressure	Decrease mean d_p	Decrease temperature
		Different Particle Size Distribution (Gaussian, Narrow)	Increase U/U_{mf} ratio
		Decrease fuel particle size	Decrease fuel feed rate
			Decrease Alkali Metal/Alkali Metal + Si content of fuel
			Use of Al/Mg/Ca-based additives
			Decrease bed material SiO_2 content (use of Al/Mg/Ca-based bed material)

1197

1198

1199 **Table 6: Summary of common agglomeration indices and relationships. Adapted and expanded upon from the work of Gatternig [98, p. 56]**

Index	Definition	Limit(s) for safe operation	Reference
Alkali Index	$AI = (K_2O + Na_2O)kg/GJ$	0.17 < AI < 0.34 Agglomeration possible AI > 0.34 Agglomeration near certain	[90, 99, 100]
Bed Agglomeration Index	$BAI = \frac{Fe_2O_3}{K_2O + Na_2O}$	Agglomeration when BAI < 0.15	[90, 119]
Base-to-acid ratio	$R_{b/a} = \frac{\%(Fe_2O_3 + CaO + MgO + K_2O + Na_2O)}{\%(SiO_2 + TiO_2 + Al_2O_3)}$	Lower $R_{b/a}$ implies lower ash melt temperatures, see [74]	[10, 74]
Agglomeration Index I1	$I1 = \frac{Na + K}{2S + Cl}$	High agglomeration potential when I1 > 1	[40]
Agglomeration Index I2	$I2 = \frac{Na + K + Si}{Ca + P + Mg}$	I2 > 1 <i>Noted as being arbitrary/requiring further confirmation</i>	[40]
Alkaline earth oxides to alkaline oxides	$I = \frac{(CaO + MgO)}{(K_2O + Na_2O)}$	No effective correlation found	[101]

1200